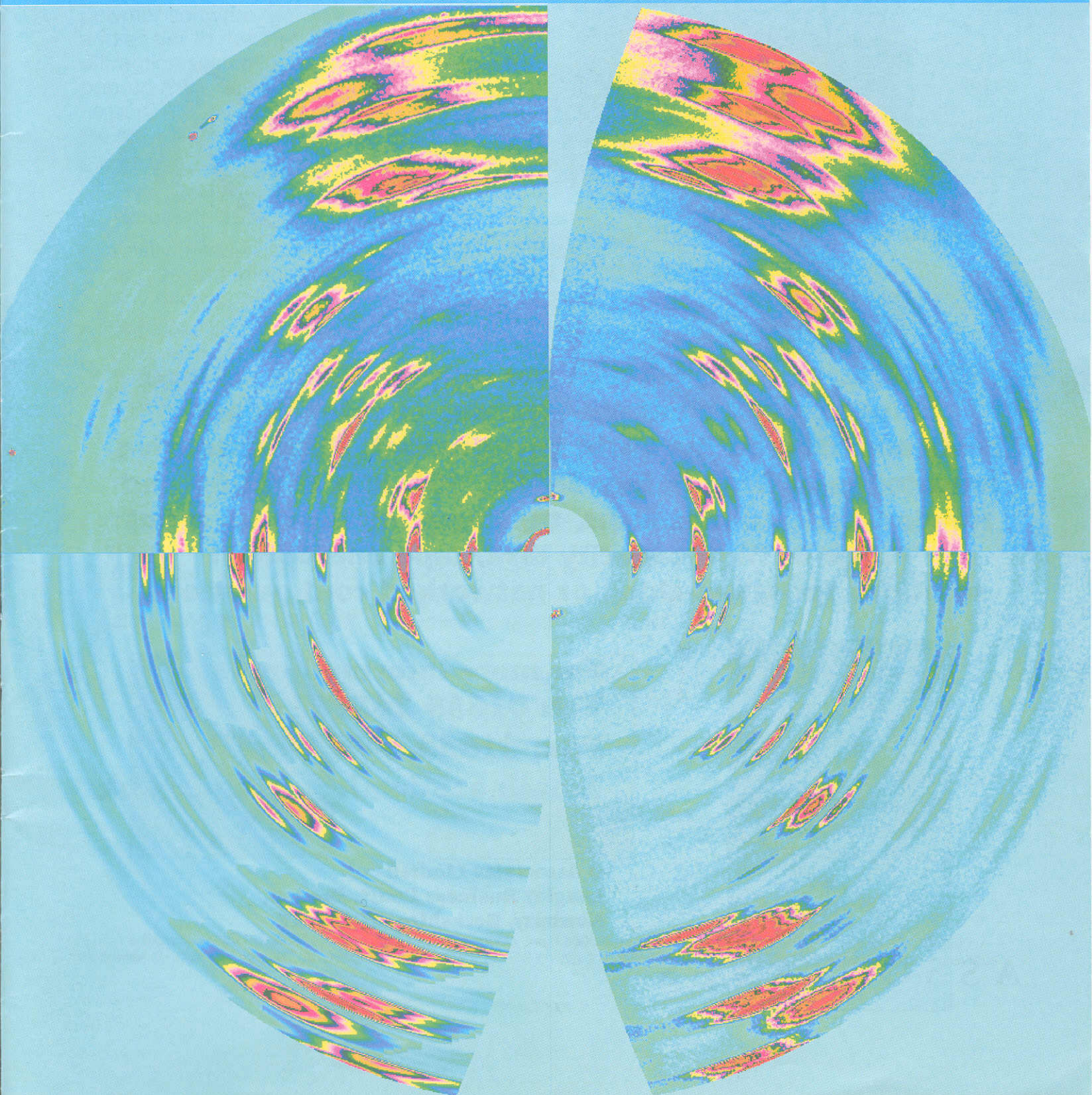


# **THE CCP13 NEWSLETTER**

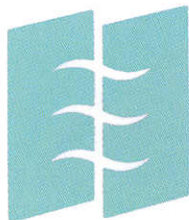
***Software Development for Fibre Diffraction***

Issue 4

December 1995



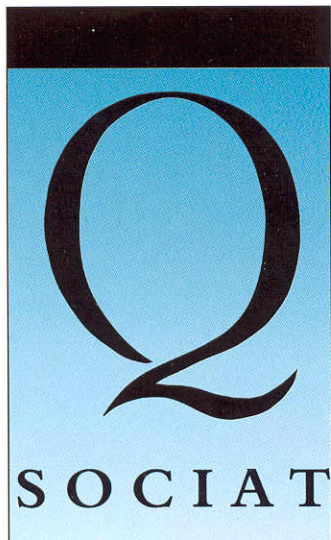
# *Specialist users require specialist data storage solutions*



LEGATO™

StorageWorks

**Q Associates specialises in the supply of data storage solutions and computer systems to research and academic users in the UNIX environment. With extensive knowledge of Digital, Sun SPARC, SGI, IBM RS/6000 and Hewlett-Packard platforms, the company provides a full range of high capacity disk, tape and optical solutions for stand-alone or networked configurations.**



**For more information:  
Tel: 01635 248181  
Fax: 01635 247616  
Email: [academic@qassoc.co.uk](mailto:academic@qassoc.co.uk)**

**Q Associates Limited  
Langley Business Court, Beedon,  
Newbury, Berkshire RG20 8RY**

# Contents

Cover .....	1
The CCP13 Committee Members.....	2
Chairman's Message.....	3
1995 ACA Meeting, Montreal: Fibre Diffraction SIG, J.Squire.....	4
Report on the 4th CCP13/NCD Workshop - May 1995, G.Mant.....	5
CCP13 and the World Wide Web, G.Mant and R.Denny.....	7
CCP13 Program Updates, R.Denny.....	8
Summary of Available CCP13/NCD Software.....	10

## Contributed Articles

Assessment of the Torus Algorithm for Global Optimization, R.Denny.....	11
A Multi-type Scatterer Implementation of the Debye Formula, E.Pantos.....	14
"imageNCIF": An Initiative to Standardise Image Format, A.Hammersley.....	14
Synchrotron Studies of Amyloid Fibrils, C.Blake.....	16
Time-Resolved SAXS Measurements on Gel Setting and Gel Melting of Triblock Copolymer Gels, K.Reynders and H.Reynaers.....	17
Small-Angle Scattering of Biological and Polymer Samples under Pressure at the ESRF, M.Lorenzen.....	18

## 4th Annual Workshop Prize - Winning Abstracts

An Actin's Eye View of Myosin: SAXS meets PX, L.Hudson, J.Harfard, R.Denny, J.Squire.....	20
Simultaneous SAXS/FT-IR Studies of Reaction Kinetics and Structure Development during Polymer processing, A.J.Ryan, J.Cooke, M.J.Elwell, P.Draper, S.Naylor, D.Bogg, G.Derbyshire, B.U.Komanschek and W.Bras.....	23
<b>1995 CCP13/NCD Annual Meeting Abstracts.....</b>	<b>25</b>

## Forthcoming Meetings

The 1996 CCP13 Workshop - May 7-9 - Daresbury Laboratory.....	34
X International Conference on Small Angle Scattering, Campinas, Brazil.....	34
The 17th IUCr General Assembly and International Congress of Crystallography, Seattle.....	34
Synchrotron X-rays in Medicine, Daresbury Laboratory.....	35
<b>CCP13 Fellowships and Visiting Scientists.....</b>	<b>36</b>

## Cover

The stages in processing a diffraction pattern from a synthetic DNA polymer are illustrated. Top-left is quadrant of the raw data, top-right shows the result of remapping this data into reciprocal space. Bottom-right shows the result of background subtraction and bottom-left shows a pattern simulated from the intensities fitted to the background subtracted data. Thanks are due to Dr. V.T. Forsyth and his colleagues at Keele University for permission to use these data.

## Newsletter Production

**Editor:** Prof. J. Squire, Biophysics Section, Blackett Laboratory, Imperial College, London SW7 2BZ

**Production:** Dr. G. Mant, Dr. R. Denny and Mr S. Eyres, CCLRC Daresbury Laboratory, Warrington WA4 4AD

**Printer:** Eaton Press, Wallasey, Merseyside, L44 7JB

## The CCP13 Committee Members

**Chairman** Prof. John Squire

Biophysics Section, Blackett Laboratory, Imperial College, London SW7 2BZ

**Phone** 0171 594 7691 **Fax** 0171 589 0191 **Email** j.squire@ic.ac.uk

**Secretary** Dr Geoff Mant

CCLRC Daresbury Laboratory, Keckwick Lane, Daresbury, Warrington WA14 4AD

**Phone** 01925 603169 **Email** g.r.mant@dl.ac.uk

**Research Assistant (Ex Officio)** Dr Richard Denny

CCLRC Daresbury Laboratory, Keckwick Lane, Daresbury, Warrington WA14 4AD

**Phone** 01925 603626 **Email** r.denny@dl.ac.uk

### Members

Dr Mike Ferenczi

National Institute for Medical Research, Ridgeway, Mill Hill, London NW7 1AA

**Phone** 0181 959 3666 **Email** m.ferenc@nimr.mrc.ac.uk

Dr Trevor Forsyth

Keele University, Physics Department, Keele, Staffs, ST5 5BG

**Phone** 01782 613847 **Email** pha23@cc.keele.ac.uk

Dr Manolis Pantos

CCLRC Daresbury Laboratory, Keckwick Lane, Daresbury, Warrington WA14 4AD

**Phone** 01925 603275 **Fax** 01925 603275 **Email** e.pantos@dl.ac.uk

Dr Rob Rule

ICI Chemicals and Polymers, Runcorn Technical Centre, The Heath, PO Box 8, Runcorn

**Phone** 01928 511437

Dr Tony Ryan

Manchester Materials Science Centre, UMIST, Grosvenor Street, Manchester, M1 7HS

**Phone** 0161 200 3614 **Email** tony.ryan@umist.ac.uk

Dr Tim Wess

The University of Stirling, Department of Biological and Molecular Sciences, Stirling, FK9 4LA

**Phone** 01786 467775 **Fax** 01786 464994 **Email** tjw3@stir.ac.uk

### Members (Ex Officio)

Dr Greg Diakun

CCLRC Daresbury Laboratory, Keckwick Lane, Daresbury, Warrington WA14 4AD

**Phone** 01925 603343 **Email** g.diakun@dl.ac.uk

Dr Rob Lewis

CCLRC Daresbury Laboratory, Keckwick Lane, Daresbury, Warrington WA14 4AD

**Phone** 01925 603544 **Email** r.a.lewis@dl.ac.uk

## CHAIRMAN'S MESSAGE

The CCP13 Newsletter continues to go from strength to strength, as befits an organisation that is healthy and making rapid progress in carrying through its aims. This edition, the fourth Newsletter, is not only bigger and meatier than ever before, but it has a new presentation format that makes it more attractive and readable and which we hope will help to promote the activities of CCP13 to a wider audience than before. Additional copies of the Newsletter have been printed so that it will go not only to people on the CCP13 mailing list, but also to places and people regarded as influential and potentially interested or supportive. In addition the Newsletters are being incorporated as part of the CCP13 World Wide Web pages (details elsewhere). The articles in the Newsletter illustrate some of the progress made in developing CCP13 fibre diffraction software in the past year, some ideas about the direction that CCP13 should take in the future, and application of the existing suite to a range of interesting biological and materials science problems. As detailed in the report by Geoff Mant, the 1995 Annual Workshop at Daresbury was, once again, a joint meeting of CCP13 and the UK Non-Crystalline Diffraction community, reflecting the considerable overlap of interests of the two groups. The meeting was very well attended and emphasises the importance of the topic. The success of the format means that the 1996 meeting will be structured in a similar way; we hope for an even larger audience. Remember not only that your poster could win a large cash prize (1st Prize - £100; 2nd Prize - £50), but also that abstracts will be included in the Annual Newsletter (also on the WWW) so that your work will be available to a much wider audience. There will be bursaries available for students and young scientists. Details of all these are given at the end of the Newsletter.

### Reminder - What is a CCP?

CCP stands for Collaborative Computational Project. CCP13 is funded in the UK mainly by the Biotechnology and Biological Sciences Research Council (BBSRC) via its "Equipment and Facilities" office. An additional grant comes from EPSRC to help fund meetings and travel for the 'synthetic polymer' side of CCP13. CCP13 is one of 12 current CCPs. These are:

- CCP1 Electronic structure of molecules
- CCP2 Continuum states of atoms and molecules

CCP3	Computational studies of surfaces
CCP4	Protein crystallography
CCP5	Computer simulation of condensed phases
CCP6	Heavy particle dynamics
CCP7	Analysis of astronomical spectra
CCP9	Electronic structure of solids
CCP11	Biosequence and structure analysis
CCP12	Novel architecture computers in Fluid Dynamics
CCP13	Fibre diffraction
CCP14	Powder diffraction

Our current CCP runs to the end of September, 1998, with support from a recent BBSRC grant. The new grant will allow the continued employment of Richard Denny as the CCP13 RA and it will provide funds towards Workshops, Newsletter production and International interactions. The funding by BBSRC and EPSRC also allows CCP13 to carry out 'good works'. At the last CCP13 Workshop it was agreed that these would be to fund a small number of 'CCP13 Travelling Fellowships' and a 'CCP13 Visiting Scientist Program', details of which are given later.

### Your Contribution

Interested groups or individuals are invited to contact any of the officers of CCP13 to obtain information about CCP13 Workshops, software developments, software standards and so on. Offers of home-written software that could be incorporated into the new CCP13 suite of programs would be much appreciated and will, of course, permanently carry the authors' attribution. Make sure that you are on the CCP13 mailing list and you will be kept informed.

### Newsletter Editorial Policy

Articles for inclusion in the CCP13 Newsletter are welcome by the Editor at any time, but preferably items for the December 1996 issue should arrive before the end of November 1996. It is hoped that the Newsletter will become an Annual 'essential' for Fibre Diffractionists. This is the place to advertise your fibre diffraction or NCD meetings, to report on new software or 'hot' results obtained using the CCP13 Suite and to provide reports of meetings of interest, preferably together with one or two photographs. All technical articles will be scrutinised both for scientific content and presentational style by

the Editor (or his nominee) together with at least one other member of the CCP13 Steering Panel. In this way we hope to maintain high standards. Remember that the Newsletter not only goes to other Fibre Diffractionists, but also to various members of the Research Council Secretariats and to other funding agencies.

### **International Cooperation**

Although these CCPs are UK funded projects, there is a very strong interest in making them international through cooperation with interested scientists in other countries. A natural link for CCP13, for example, exists with the Special Interest Group (SIG) in Fibre Diffraction of the American Crystallographic Association and possibly with some American synchrotron users (CHESS). Others exist with the ESRF at Grenoble and with the Photon Factory in Japan.

### **Retirements and New Elections**

At the 1995 Annual Meeting, Trevor Forsyth and Mike Ferenczi were re-elected as committee members and Tim Wess was elected in place of Keith Meek who retired. The services of Keith during the start up phase of CCP13 have been much appreciated and it is a pleasure to record our thanks to him for his interest and enthusiasm.

Please note that the periods of office of John Squire (Chairman), Geoff Mant (Secretary) and Manolis Pantos (committee member) will finish at the May 1996 Meeting. Any nominations for election to these posts should be sent to the CCP13 Secretary, Dr. Geoff Mant before the May meeting. All three people are willing to continue in these roles for a further 3 year period. Elections will be held at the business meeting at the CCP13/NCD Annual Workshop in May, 1996.

John Squire

### **IF YOU ARE A FIBRE DIFFRACTIONIST STUDYING SYNTHETIC OR BIOLOGICAL POLYMERS. THIS CCP IS FOR YOU. PLEASE HELP TO MAKE IT WORK!**

### **ACA MEETING - MONTREAL - JULY 23-28, 1995**

The 1995 version of the annual ACA Meeting was held in the well-appointed Palais des Congrès in Montreal, Canada. I was there as part of the session organised by the Fibre Diffraction 'Special Interest Group' (SIG) of the ACA. This was my first visit to Montreal and I had not realised until I got there quite how French it is. Although I soon realised that most people speak English, it obviously was diplomatic to exercise, at least initially, a little of the rather rusty schoolboy French that still remained. Fortunately I arrived in Montreal a day before the meeting started and was able to enjoy some of the splendid sites in this beautiful city, including a very pleasant, albeit short, cruise along the St. Lawrence River.

The Fibre Diffraction SIG meeting was divided into four sessions and was a good mix of synthetic and biological polymer work. Speakers or co-authors included some old friends from CCP13 meetings such as H. Zachmann, Watson Fuller, Alan Windle and Bill Stroud, together with some key US fibre diffractionists such as Gerald Stubbs, Rick Millane, Tom Hendrixson, John Blackwell, R. Chandrasekaran and Dan Kirschner. Another old

friend, Don Caspar, also appeared in the audience for some of the sessions. Although it was a relatively small meeting for fibre diffractionists, many of the talks were very interesting and useful and it was certainly good to renew old contacts and to make new ones. At the same time, some other parallel sessions (e.g. on small-angle scattering, neutron scattering and macromolecular structure) brought other friends to Montreal, including Trevor Forsyth in the neutron scattering session.

This was the centenary ACA meeting of the discovery of X-rays by Røntgen, so one of the sessions paid tribute to the importance to all of us of this discovery. It was also the first ACA meeting since the deaths of two great crystallographers, Dorothy Hodgkin and Linus Pauling, so on the Tuesday evening there was a special tribute to them and to the enormous contributions that they made to the subject. Some of the families and long time friends of these two scientific giants were there and made their own contributions, the whole session being both fascinating and, at times, very moving.

As a general comment on my assessment of the fibre diffraction part of the meeting, it was very clear that even on an international scale the fibre diffraction community is relatively small compared with, say, our macromolecular crystallography colleagues. On the other hand, we still have a great deal to learn about getting our act together, about cooperating and informing each other of what is going on and in making sure that internationally we really are a community. Of key importance for the good of our subject is

therefore the need not only to advertise organisations such as CCP13 as widely as possible, something that I tried to do, of course, in Montreal, but also for CCP13, the ACA SIG and other groups in other countries to coordinate their efforts in some way in order to promote as fully as possible what is a very important area of study.

John Squire

## 4th Annual CCP13/NCD Workshop

The fourth annual workshop for the collaborative computational project for fibre diffraction (CCP13) and non-crystalline diffraction (NCD) was held at Daresbury on the 9th-11th of May attracted 75 participants. The meeting was partially sponsored by Q-Associates, Siemens and Organised Computer Systems.

To reflect the joint nature of the workshop a diversity of topics, including synthetic polymers, hardware sources and detectors, software developments and biological systems, were covered. Each session began with an eminent keynote speaker, followed by presentations from specialists in the field, which included participants from not only the UK but also Belgium, France, Germany, Holland and the USA. A new feature this year was a series of short presentations (no more than 3 minutes), by students, on the content of their posters. The talks were complemented by a poster session and a commercial exhibition by the sponsors Q-Associates, Siemens and Organised Computer Systems.

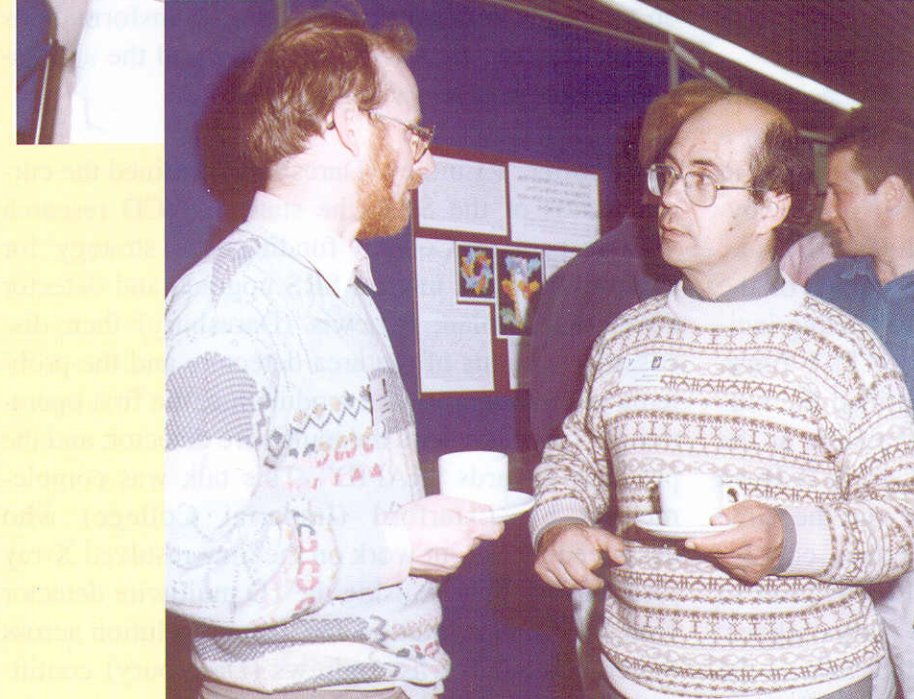
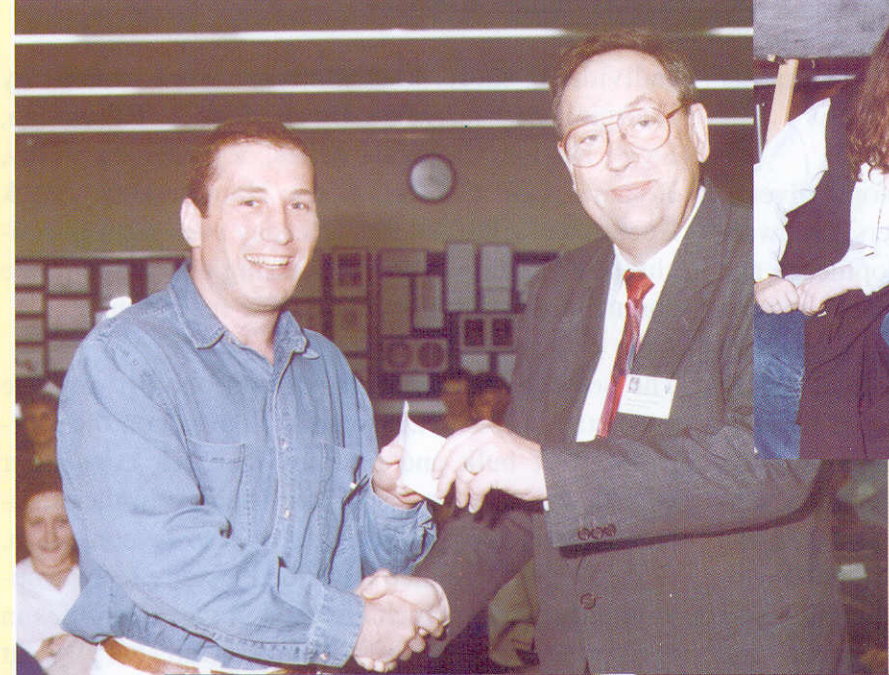
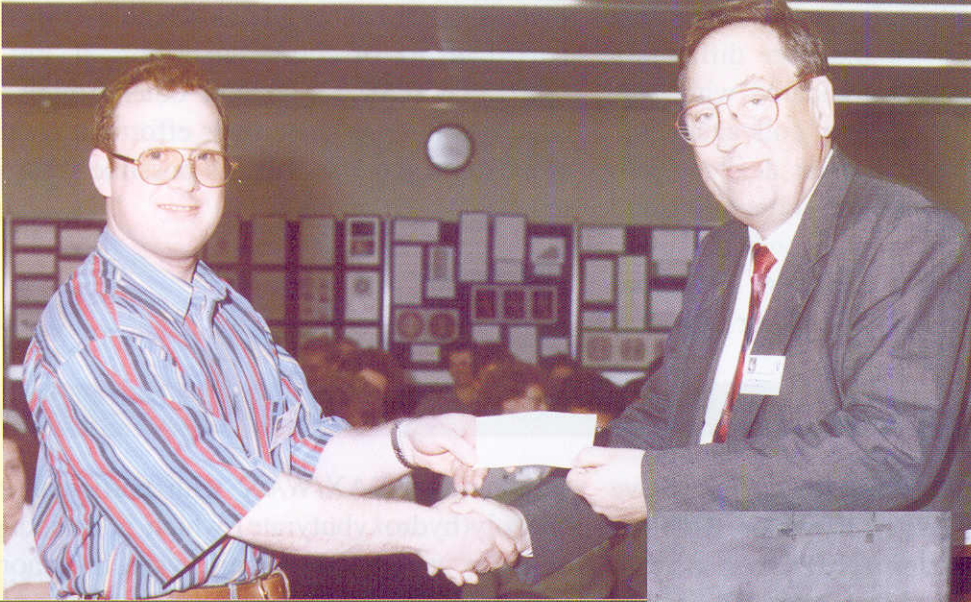
After the Chairman's introduction G.Zachmann (Hamburg) opened the polymer session by giving a general introduction to polymers, before going on to describe work on spinning/extrusion of polypropylene, SAX/WAX studies of polyvinylidene fluoride, liquid crystalline polymer dislocations studied on the micro-focus beamline at the ESRF and grazing incidence (30Å depth into layer) studies of PET films. B.Komanschek (Daresbury) then described the current facilities, for polymer studies, available at the SRS, primarily on stations 8.2 and 16.1. A.Ryan (UMIST) described his latest work on the time resolved SAX/DSC crystallisation block copolymers, in particular PBO-PEO and PEE-PE head to tail polymers where only half crystallises. R.Cameron concluded the session with a talk on the phase transitions of natural polymers studied by

simultaneous SAX/WAX with particular emphasis on Poly(hydroxybutyrate) which is a biodegradable polymer which has semi-crystalline morphology (spherulite).

Individual short presentations were made by Georgina Bryant, Mike Ewell, Patrick Fairclough, Steve Naylor, Catherine Miles, V. Balaguraswamy, Richard van Gelder, Andy Hammersley, Mark Boehm and Alun Ashton. Tuesday evening was concluded with dinner, poster viewing and judging, the commercial exhibition and a wine reception.

The second day commenced with another keynote presentation from H.Reynaers (Leuven) on the morphology of bulk and oriented tri-block copolymer gels in which he described the changes in the structure on stretching from a spherical to layered form. G.Tiddy (Salford) then described a study of lyotropic liquid crystals which are used in vast quantities in the surfactant industry. E.Pantos (Daresbury) went on to discuss his recent work on gel transformations studied by SAXS, SANS and NMR and the simulation of the processes using fractals.

After coffee, P.Lindley (Daresbury) outlined the current status of the SRS, the state of NCD research with respect to Council funding, the strategy for Diamond and the interim SRS upgrade and detector development plan. R.Lewis (Daresbury) then discussed the status of the area detectors and the problems of the detector wire modulation, the first operational experience with the multiwire detector, and the progress towards "RAPID". This talk was complemented by J.Harford (Imperial College) who described the recent work on the time resolved X-ray study of fish muscle using the 1D multiwire detector with 1ms time resolution and 1mm resolution across the equator. E.Towns-Andrews (Daresbury) continued the hardware theme with a talk on recent results



**Top and Centre Left:** Mike Elwell and Richard Denny (on behalf of Jeff Harford) receive cheques as joint winners of the prize for best poster from Gerhard Zachmann

**Centre Right:** Anthony Gleeson points out his favourite dish on the evening menu to Catherine Miles.

**Bottom:** Goran Ungar and Rob

and developments on SRS station 16.1, highlighting in particular three experiments: firstly, the 20mS time resolved studies of muscle by M.Ferenczi, secondly, the slitted beam work of J.Squire utilising an A3 image plate to record the 59Å reflection of fish muscle and lastly the insect flight muscle work of M.Reedy. M.Lorenzen (ESRF) then described the development of a high pressure cell for use on the micro-focus and high brilliance beamlines at the ESRF, highlighting its use with recent results on tri-block gels. T.Irving (Chicago) rounded up the session by outlining the plans for the BioCAT (Collaborative Access Team) beamline at the Advance Photon Source.

After coffee the poster prizes were awarded. The judges (P.Lindley and G.Zachmann) deliberation was to award a joint first place prize to J.Harford *et al* (Imperial College, London), a cheque for £75, for their poster "Muscle the Movie", and for the second year in succession to M.Elwell (UMIST) for his poster "Simultaneous SAXS/FTIR".

R.Rule (ICI) opened a short session on software by describing the modelling of SAXS patterns of polyurethane utilising correlation functions. He also stressed the importance of error correction, with particular reference to beam intensity measurements and scaler overflow. R.Denny (Daresbury/Imperial College) then described the progress on the CCP13 program suite, outlining the developments in the programs FIX, TBACK, LSQINT, SAMPLE and DECONV.

J.Bordas (Liverpool) discussed the effect of the anti-tumor drug, taxol, on the assembly of tubulin as studied by turbidity and SAXS and also the effect of vinblastin as observed by cryoelectron microscopy (EM), highlighting the relationship between EM and

SAXS. C.Blake (Oxford) finished the afternoon with a talk on amyloidosis caused by an aggregation of proteins to form fibrils, as studied by X-ray diffraction, which have been implicated in diseases such as Alzheimers, type II diabetes and BSE. The second day concluded with a sherry reception and conference dinner at Daresbury.

The final day started with M.Reedy discussing his latest work, hot from the beamline, on the time resolved structure of insect flight muscle contraction, complementing this with electron microscopy studies. M.Ferenczi (NIMR) described some recent developments in the time resolved x-ray diffraction of single muscle fibres, using stepped length changes with stretch and release and also permeabilised fibres using alpha-toxin. D.Marvin (Cambridge) then outlined the maximum entropy method in the study of Filamentous Bacteriophage. The structure is rod like alpha-helix when magnetically aligned, multiple calculations were then performed selecting the best fits. W.Fuller (Keele) showed a video of the instrumentation and results of the development of crystallinity recorded on the micro-focus beamline at the ESRF. The meeting was rounded off with presentations from P.Langan on neutron studies on the D19 beamline at the ILL, S.Perkins (Royal Free Hospital) on the automated curve fitting of SAXS data of multidomain proteins and lastly W.Bras (AMOLF) on the magnetic alignment of microtubules.

The workshop concluded with a special vote of thanks to Val Matthews and Vanessa Porter for all the hard work and organisation that went into making the whole meeting run smoothly.

Geoff Mant

## CCP13 and the World Wide Web

The huge growth of the Internet as a mechanism for the rapid dissemination of information has led to the creation of the CCP13 website. The CCP13 home page (Figure 1) is available from the URL:

<http://www.dl.ac.uk/CCP/CCP13>

The home page currently points to six areas of information, a general introduction, the committee, workshops, newsletters, software and publications. To date, all of the previous workshop abstracts and newsletters have been digitised and converted to WWW viewable documents. We hope that, from this

year on, submissions to the CCP13 workshop and contributions to the newsletters will be submitted electronically.

The latest addition to our pages is the CCP13 license form and program retrieval mechanism (see Figure 2). Basically, all subscribers are requested to enter their name and E-mail address and select the desired program and operating system on which it will run. Selection of the retrieve link on the subsequently displayed page will transfer a compressed executable version of the program to a directory you specify.

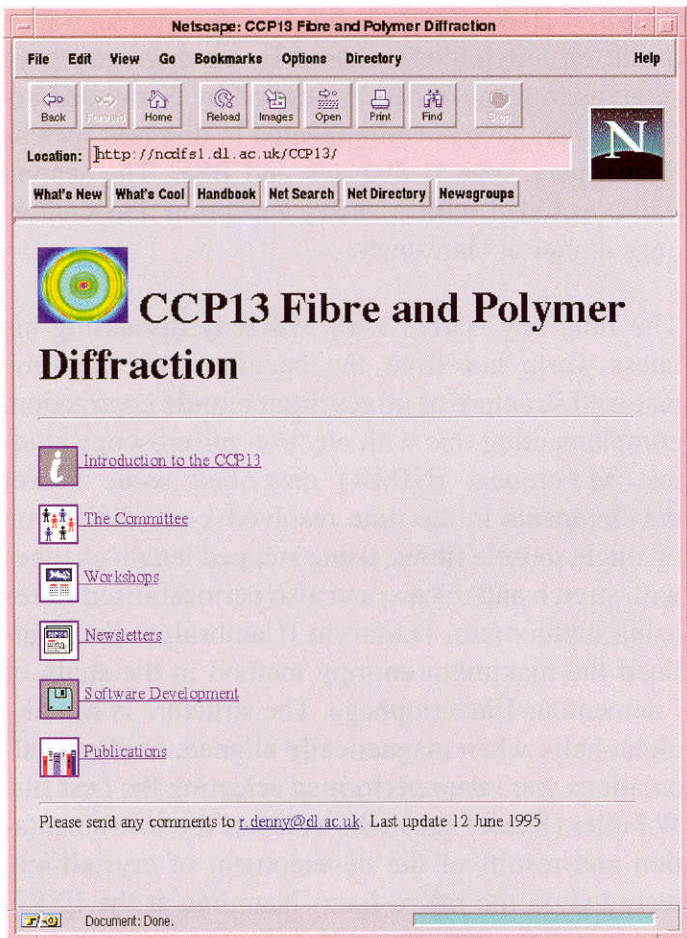


**Figure 1** The CCP13 WWW home page displayed with the Netscape program.

**Figure 2** The CCP13 WWW License and program retrieval request form. Look out for three forthcoming forms within the workshop96 index to register yourself for the CCP13 workshop 7-9th May, to submit an abstract and apply for a bursary.

## CCP13 Program Updates

### Richard Denny

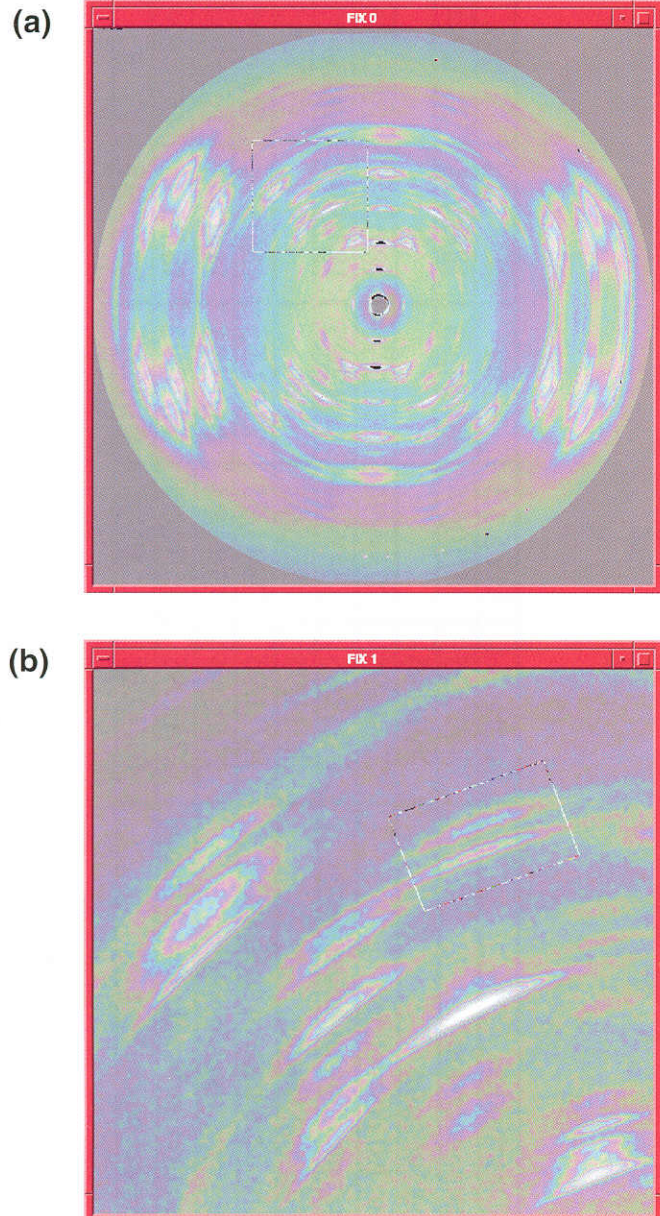
Biophysics Section, Blackett Laboratory, Imperial College,  
London SW7 2BZ  
&  
CCLRC Daresbury Laboratory, Warrington, Cheshire WA4  
4AD

**FIX** Updates include the use of backing store to restore window contents after exposure events and a refresh command to repaint images where the lines, crosses, etc. drawn by FIX are unwanted. The thresholds for an image can now be modified at any time, not just when the image is first generated. A thickline command has been added for integration of data in rectangular regions in general orientations. The collapsed data which results from the integration can then be fitted in the normal way with the line command (see figure 1). The line fitting routines are now common with those used in FIT so that development will be common to both programs.

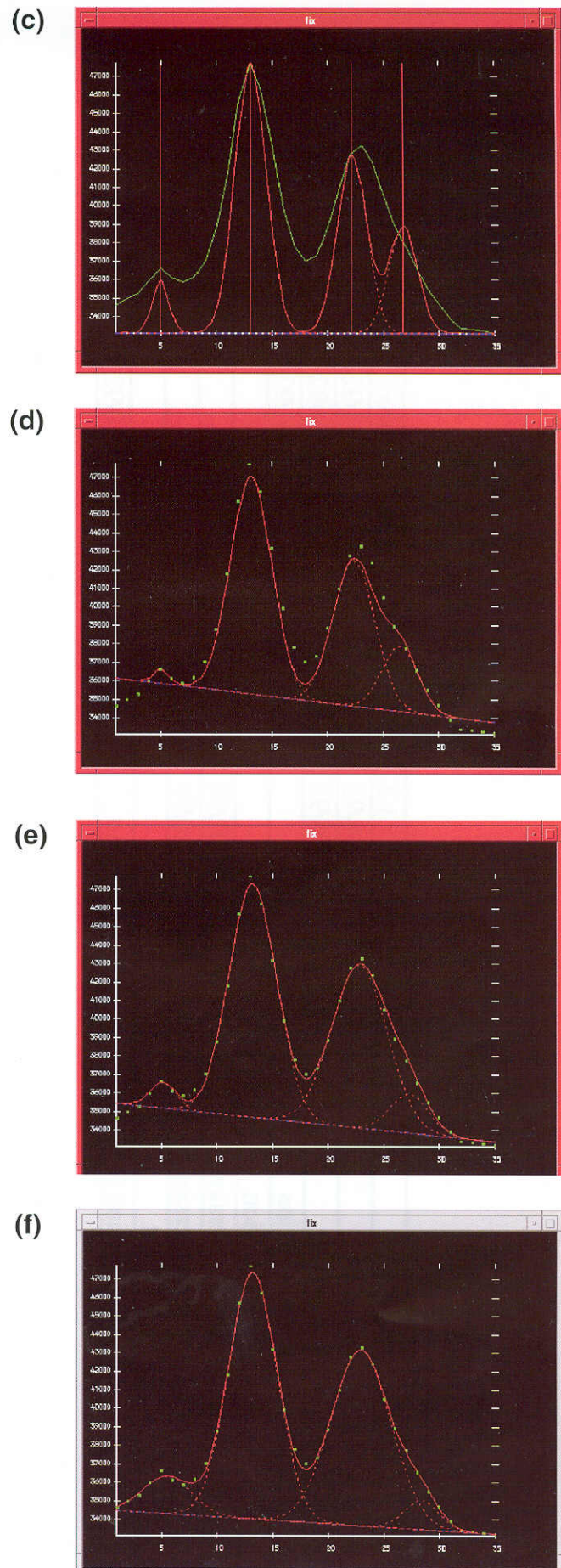
**FIT** Five peak functions are now supported: Gaussian, Lorentzian, Voigt, Pearson VII and the Debye formula for diffraction from chain molecules. Simple lattice constraints can now be enforced on the positions of peaks for tetragonal or hexagonal lattice types where the  $l$  index is constant. General cubic indices will be allowed for in the near future. Also, simple limits can be placed on the range of a parameter during refinement. It is also now possible to step through the refinement algorithm, one iteration at a time, changing the value of any parameter when desired. Versions of the routines used in FIT have now been written which utilize PGPLT line graphics for portability to machines which do not have the GHOST80 graphics library installed. This is an interim measure while a graphical user interface is developed.

**LSQINT** This program is in genuine need of updating as many modifications have been tacked on for different users. Work is currently in progress to replace the four available profile types with a single,

**Figure 1** An illustration of the use of the thickline command in FIX and the subsequent line fitting using the step option. (a) shows a window containing the diffraction pattern from the A form of DNA. A rectangular region has been selected for enlargement using the box command. In (b), the window displays the enlarged section in which a rectangular region has been selected for integration across its width using the thickline command. Once the line fitting part of the program has been entered, an initial set of peak parameters can be chosen as shown in (c). In (d) and (e) the results of successive iterations of the fitting procedure are shown, generated by the step command. In (f), the final model, achieved after 7 iterations, is shown.



more flexible, form. The single precision least-squares fitting option will be removed, but an option to use a version of the maximum entropy fitting which is more economical with memory will be included. The ability to integrate intensity from multiple lattices introduces the possibility of more parameters into the cell and profile refinement algorithm so the downhill-simplex method used for the refinement will be replaced by a modified version which



partitions the parameters into groups based on the magnitude of their shifts. All mathematical routines and matrix operations will use the SLATEC and LAPACK libraries.

## Summary of Available CCP13/NCD Software

Program	Program Description	Solaris 2.4	Irix 5.1.3	HPUX	IBM AIX	Ultrix	OSF	Linux
<b>xotoko</b>	1-D data manipulation	13/10/95	07/08/95	24/06/92	-	13/04/92	-	-
<b>bsl</b>	2-D data manipulation	06/10/95	07/08/95	27/06/92	-	13/04/92	-	-
<b>v2a</b>	vax to unix data conversion	19/05/95	-	27/06/92	-	13/04/92	-	-
<b>a2v</b>	unix to vax data conversion	19/05/95	-	-	-	-	-	-
<b>otcon</b>	ascii to otoko data conversion	0/06/95	08/07/94	-	-	-	-	-
<b>reconv</b>	otoko to ascii data conversion	06/06/95	31/10/94	28/06/92	-	-	-	-
<b>tiff2bsl</b>	image plate to bsl format	06/06/95	-	-	-	-	-	-
<b>i2a</b>	ieee to ansi data conversion (DEC only)	n/a	n/a	n/a	n/a	09/10/92	-	-

Program	Program Description	Solaris 2.4	Irix 5.1.3	HPUX	IBM AIX	Ultrix	OSF	Linux
<b>conv</b>	file format conversion	24/10/95	31/10/94	05/04/95	18/05/95	31/10/94	10/10/95	
<b>corfunc</b>	correlation function	26/10/95						
<b>fd2bsl</b>	intensity to bsl conversion	23/06/95	27/04/94	01/12/95	18/05/95	20/08/93	28/09/95	
<b>fdscale</b>	scaling and merging of intensities	01/12/95	13/06/94	01/12/95	18/05/95	20/08/93	28/09/95	
<b>fit/pgfit</b>	1-D plotting and fitting	08/11/95	15/05/95			17/09/95		
<b>fix/pgfix</b>	preliminary fibre pattern analysis	16/11/95	20/11/95	29/11/95	18/05/95	20/09/95	20/09/95	
<b>storec</b>	reciprocal space transformation	23/06/95	25/11/94	01/12/95	11/07/95	04/02/94	26/01/95	
<b>lsqint</b>	2-D integration and background fitting	23/06/95	25/11/94	27/10/95	18/05/95	02/12/94	24/03/95	24/09/95
<b>sample</b>	Fourier-Bessel smoothing	01/12/95	15/05/95	01/12/95	24/05/95			

The tables above list the currently distributed CCP13/NCD programs, available as executable modules. The dates refer to the last creation of the executable.

## Contributed Articles

### Assessment of the Torus Algorithm for Global Optimization

Richard Denny

Biophysics Section, Blackett Laboratory, Imperial College,  
London SW7 2BZ  
&  
CCLRC Daresbury Laboratory, Warrington, Cheshire WA4  
4AD

Methods for global optimization of a parameter set as judged against some objective function are particularly relevant to the problem of optimizing a model against a set of diffraction data. There are many methods available for refining a model once in the neighbourhood of the desired minimum which take only downhill steps. However, methods which can escape the neighbourhood of a local minimum and locate the best solution are less common, an example being a simple grid search. This is usually too expensive in terms of the number of function evaluations required for problems involving more than a few variables. Other methods include simulated annealing and the so-called genetic algorithms.

The Torus algorithm (Rabinowitz, 1995) is a stochastic method which uses only function evaluations, no derivative calculations are required. The algorithm employs random shifting of variables within two different schemes for limiting the maximum range of those shifts. Initially, the ranges of the variables are defined by lower and upper bounds supplied by the user. Thereafter, in the controlling function, the variables are sequentially bumped around the set which currently gives the lowest function

value, the range of the bumps decreasing exponentially with a low decay constant (slow cooling). The controlling function calls two routines for minimizing the objective function about the bumped variable set, one which applies random shifts to all variables and one which applies shifts to only one variable at a time. Both these routines reduce the maximum range of the shifts logarithmically (rapid cooling) from the ranges modified by the controlling function. The shifts are also constrained by a cutoff value for each variable supplied by the user. In the controlling function, a multiple of the cutoff value is used as the minimum size of the range. In the minimization routines, the cutoffs provide the minimum magnitudes of the random shifts. Therefore, the cutoffs can be thought of as defining minimum starting and finishing temperatures for the minimization routines. The implementation of this method investigated here was written in C from pseudocode published in Rabinowitz (1995).

A simple function with many local minima was used to investigate the efficacy of the Torus algorithm,

$$f_{n,k}(x) = \sum_{i=1}^n x_i^2 + k \left( 1 - \prod_{i=1}^n \cos x_i \right)$$

where  $n$  is the number of dimensions and  $k$  is a weighting factor between the quadratic term which defines the global minimum and the periodic term which introduces the local minima. It is clear by inspection of the function that the global minimum has a value of 0 and is situated at  $x_i=0$  for  $i=1,n$ . The family of next lowest minima have a value of

$n, k$	TORUS			REPLEX	
	No. of global minima	Av. global minimum	Av. no. of function calls	Av. global minimum	Av. no. of function calls
2 , 400	15	26.99	8054	$5.47 \times 10^{-9}$	120
2 , 200	32	19.14	8104	$5.01 \times 10^{-9}$	114
2 , 100	49	9.35	8585	$4.93 \times 10^{-9}$	100
10 , 400	14	0.013	143082	$1.79 \times 10^{-6}$	592
10 , 200	26	7.34	149014	$3.52 \times 10^{-6}$	607
10 , 100	47	5.52	156182	$1.14 \times 10^{-4}$	591

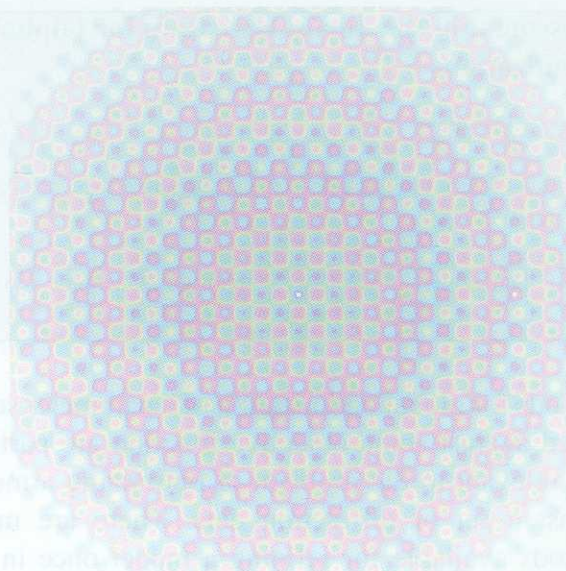
**Table 1** Each combination of  $n$  and  $k$  was tested 100 times. The averages of the number of functions calls were calculated over all trials, not just those in which the neighbourhood of the global minimum was located.

approximately  $2\pi^2$  and occur when two of the  $x_i = \pm\pi$  and the rest are equal to zero. The starting set for each trial consisted of  $x_1=12\pi$  and  $x_i=0$  for  $i=2,n$  with the range for each variable being  $-50 \leq x_i \leq 50$ . The cutoff value applied for each dimension was  $\Delta x=0.01$ . A representation of the function is shown in figure 1. Control parameters for the algorithm were left at their default values.

Each test consisted of 100 trials of the algorithm for a particular  $n$  and  $k$ . In order to clearly identify the neighbourhood of the local minimum into which the result of the Torus algorithm fell, each application was followed by refinement by a modification (REPLEX) of the downhill simplex method (Nelder & Mead, 1965), in which the variable set is partitioned to form groups with similar shifts. The results of these tests are summarized in table 1. The results of the trials for  $n=2$  are shown graphically in figure 2.

As can be seen from table 1, the Torus algorithm requires far more function evaluations than the downhill simplex method to reach convergence. However, it has the great advantage that in a fair proportion of the trials, it successfully locates the neighbourhood of the global minimum, whereas, from the same starting point, the downhill simplex method would barely move. The downhill simplex method comes into its own when used to refine solutions suggested by the Torus algorithm. One can also compare the efficiency of the algorithm to a grid search in increasing the dimension of the problem. The scaling of the number of function evaluations for  $n=2$  to  $n=10$  is approximately 18 with little or no loss of efficiency in finding the global minimum. The number of function evaluations required by a grid search for  $n=10$ , assuming the same number of evaluations as the Torus algorithm for  $n=2$  (corresponding to a step size of 1.13 in each dimension), is approximately  $3.3 \times 10^{19}$ , a scaling of  $4.1 \times 10^{15}$ . Even though the Torus algorithm cannot guarantee to locate the global minimum, it seems to offer a considerable advantage over a grid search for a problem of more than 1 or 2 dimensions. As with any non-trivial method of finding a global minimum, the algorithm has a number of control parameters which can be tuned to suit the problem at hand. This tuning is in itself a tricky optimization problem which has not been explored here.

(a)



(b)

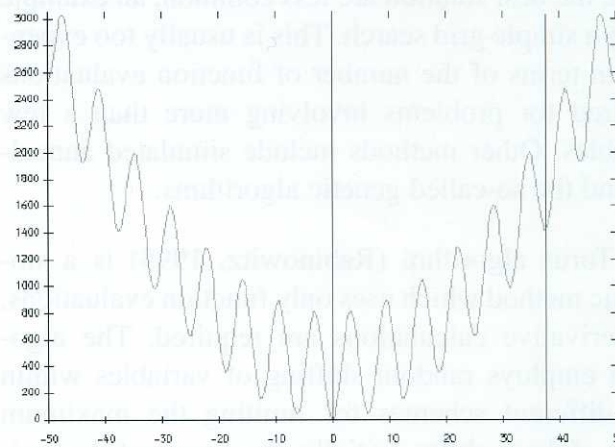


**Figure 1** (a) shows a colour-contour representation of the test function for  $n = 2$ ,  $k = 400$ , the limits in both dimensions being  $-50$  to  $50$ . The central global minimum is marked with a white dot as is the starting point to the right of the centre. (b) shows a slice through the centre of the surface with  $x_2 = 0$ . The central global minimum and the starting point are marked with vertical lines.

## References

- Rabinowitz F.M. 1995. Algorithm 744: A stochastic algorithm for global minimization with constraints. *ACM Trans. Math. Softw.*, **21**, 194-213.
- Nelder, J.A. and Mead, R. 1965. A simplex method for function minimization. *Comput. J.*, **7**, 308-313.

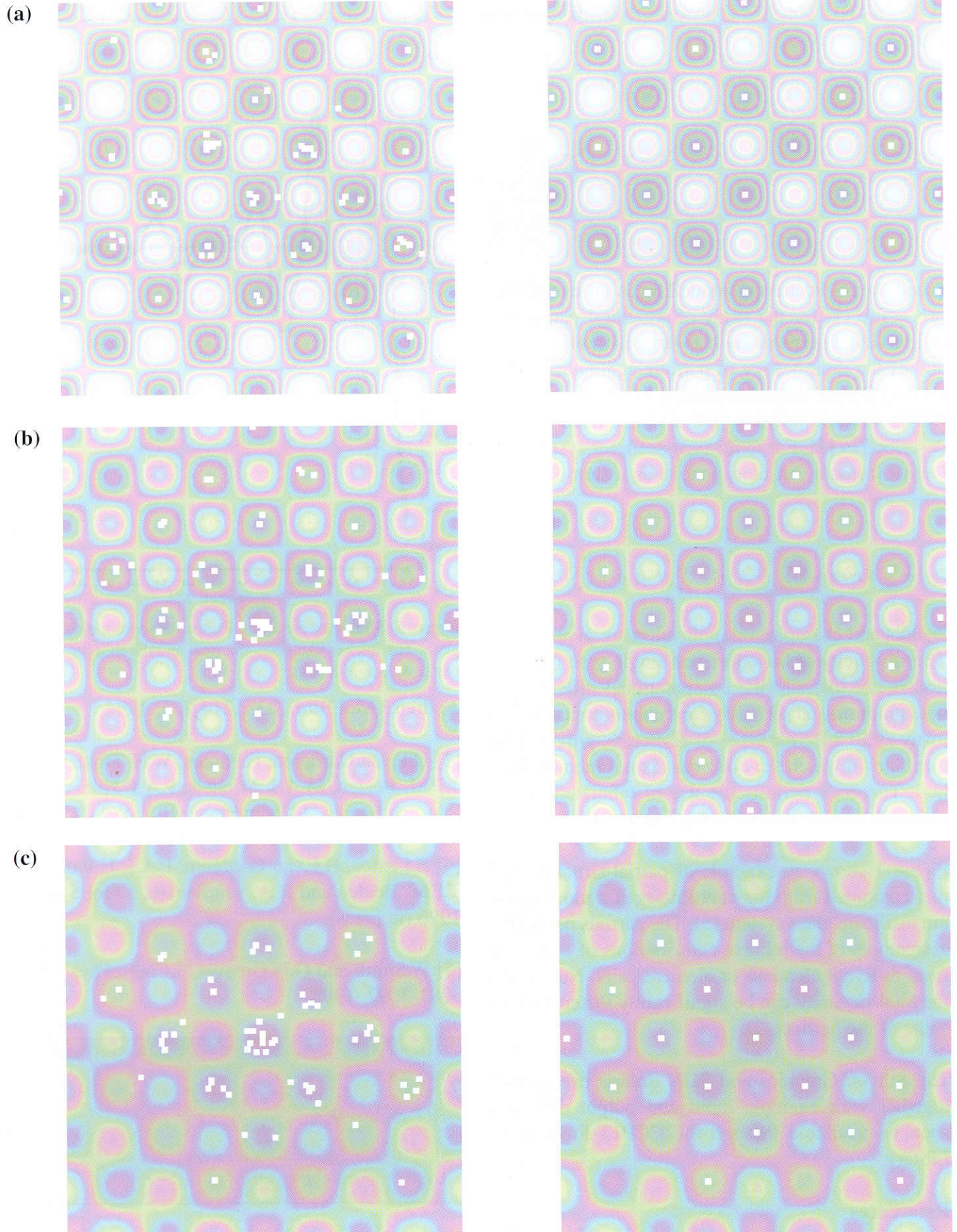


**Figure 2** This shows the results of the trials for  $n = 2$ . The central portion of the function surface is shown ( $-4\pi < x_1, x_2 < 4\pi$ ) with the resulting coordinates of the Torus algorithm on the left and the subsequent downhill simplex refinement on the right. (a)  $k = 400$  (b)  $k = 200$  (c)  $k = 100$

## A Multi-type Scatterer Implementation of the Debye Formula.

Emmanuel Pantos<sup>1</sup>, H.F. van Garderen<sup>2</sup> and P.A.J. Hilbers<sup>2</sup>

<sup>1</sup>CLRC, Daresbury Laboratory, Keckwick Lane, Warrington WA4 4AD, United Kingdom

<sup>2</sup>Eindhoven University of Technology, P.O. Box 513, 5600 MB Eindhoven, The Netherlands.

Small Angle Scattering modelling is an established procedure [1] for the study of structural parameters of individual particles such as large biomolecules [2] and of the morphology of particle aggregates [3]. A CPU-efficient implementation of the optimised Debye formula utilising pair distance histograms is described in [1]. For multi-type scatterer systems the Debye formula can be expanded as a sum of partial intensities

$$I(q) = \sum_{i=1}^{N_{types}} N_i F_i^2(q) + 2 \sum_{i=1}^{N_{types}} \sum_{j=i}^{N_{types}} I_{ij}(q) = \sum_{i=1}^{N_{types}} \left[ N_i P_{ii}(q) + 2 \sum_{j=i}^{N_{types}} P_{ij}(q) S_{ij}(q) \right]$$

Details and examples of application are given in [4]. The simplicity of the optimised single-type formulation is not lost and the computational efficiency is not compromised seriously for systems containing as many as 10 different types of scatterers, provided the machine on which the code runs is not memory limited. The code permits the use of tabulated atomic structure factors, instead of hard sphere form factors.

Figure 1 shows an example of partial structure factors computed from the coordinates of a model sodium disilicate glass system [5]. The partials permit the assignment of the relative contributions of scattering from different elements or element pairs. Notice that the total intensity can be significantly different from some of the partials.

The Silicon Graphics and SUN Solaris executables together with example input and output data will soon be available through the CCP13 Programme Library.

## References

- [1] H.F.van Garderen, E.Pantos, W.H Dokter, T.P.M Beelen, and R.A.van Santen, Mod.Sim.Mat.Sci.Eng., 2, 295-312, 1994.
- [2] J.Diaz, E.Pantos, J.Bordas and J-M

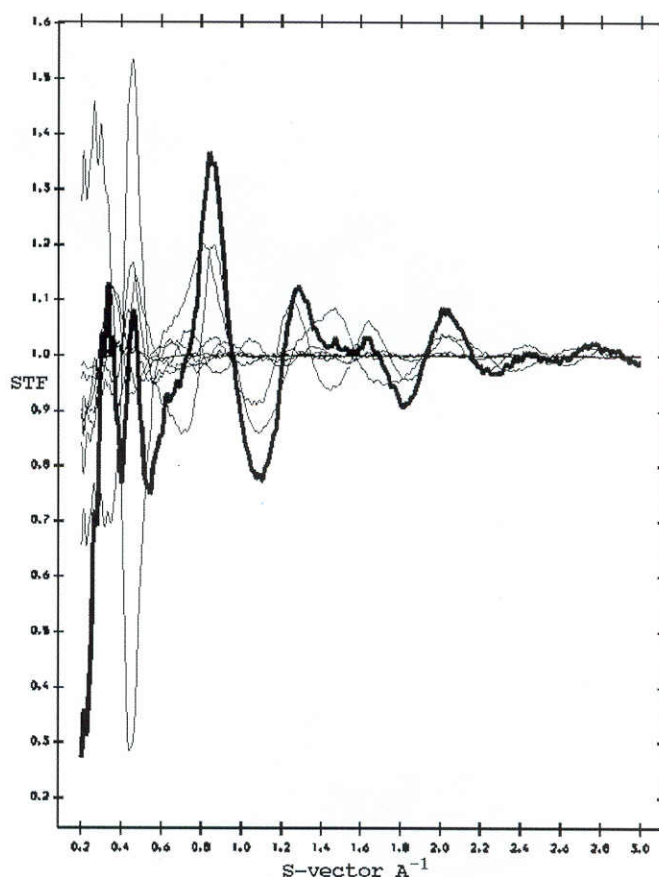


Figure 1. Simulated Structure Factor for sodium disilicate glass. The thicker line gives the total and the thin lines the partial structure factors.

Andreu, J.Mol.Biol., 238, 214-225, 1994.

[3] H.F.van Garderen, E.Pantos, W.H. Dokter, T.P.M. Beelen, M.A.J. Michels, P.A.J. Hilbers, and R.A.van Santen. J.Chem.Phys., 102, 480-495, 1995.

[4] E.Pantos, H.F.van Garderen, P.A.J. Hilbers, T.P.M. Beelen and R.A. van Santen, J.Mol.Struct. 1996 (in press).

[5] W.Smith and G.N.Greaves, J.Chem.Phys. 103, 3091-3097, 1995.

## "imageNCIF": An Initiative to Standardise Image Formats"

A P Hammersley,

ESRF, BP 220, 38043 Grenoble Cedex, France.  
E-mail: hammersley@esrf.fr

## Introduction

Data formats and in particular image formats are a problem! Most scientists will know the problem of having to find or write a conversion program, to convert a file in a particular format to a format which can

be input to the analysis program which they want to use. Similarly application programmers will know the problem that however many formats they support, there will always be new detectors with new data formats which will be required.

If a sufficiently versatile common format was widely adopted this “Babylon” of formats would at least be limited and maybe the number would eventually decrease. Initiatives to define such formats are not new, but for storage of large quantities of experimental data there has been no commonly adopted format to date. For the task of passing more limited quantities of processed, typically structural, data amongst the crystallographic community, a common standard format has been defined: “CIF” [1]. “CIF” stands for “Crystallographic Information File”, and is an ASCII text based, flexible and extensible human readable archive file format.

In March 1995 a computing workshop was organised at the Brookhaven National Laboratory concentrating on the use and design of “Graphical User Interfaces” (GUI’s). One subject area which was clearly of general common interest was image formats.

A working group was formed and time was dedicated to an open discussion on the requirements of such a format. It was here (to my knowledge) that the idea of extending the CIF-concept to define the header information for images was first discussed by a sizeable group.

## What is CIF?

CIF is a standard format maintained and “owned” by the International Union of Crystallography (IUCr) for archiving and transporting crystallographic data [1]. One important current use is the submission of papers on structure determinations to Acta Crystallographica Section C.

The format consists of simple ASCII text keyword and keyword value pairs. A large “dictionary” defines the keywords and possible values. There is support for comments, for multi-line character text, and for structuring separate data sections. The keywords are defined from a hierarchical “class” (data name categories) and “sub-class” system. e.g. All keywords which start with \_diffrn refer to data from diffraction measurements. A typical line from a CIF file, which could also be relevant to an experimental image file is:

```
_diffrn_radiation_wavelength 0.76 #This  
is 16.3 keV
```

Importantly, the dictionary defines the precise meaning of the data names, and the units and valid range when appropriate.

A number of software tools are available from the IUCr to work with CIF’s, and libraries are available to help read and write CIF’s. CIF is maintained and extended through the IUCr COMCIFS committee. At present there are initiatives to extend CIF (Core dictionary) to cover the extra needs of macromolecular crystallography (mmCIF) and powder diffraction.

For more information on CIF, there is a World-Wide-Web page with links to associated pages (<http://www.iucr.ac.uk/cif/home.html>).

## What is “imageNCIF”?

“imageNCIF” (= image (Not) CIF; cf. mmCIF), is an E-mail based working/discussion group working on the idea of extending the CIF concept to cover the storage of experimental data, and in particular 2-D “image” data. There are presently about 15 members of this group, which contains representatives from commercial detector manufacturers, programmers of data analysis software, members concerned with data acquisition at user facilities, and crystallographers from a variety of different scientific disciplines.

The aim is to standardise the passing of image and associated crystallographic experimental data from one institute to another, one make of computer system to another, and from one computer program (acquisition or analysis) to another. It is desirable that the image file contains the necessary associated experimental information to make data processing as automatic as possible.

The basic aim is essentially the same as that of CIF, but the difference in the quantities of data involved mean that there is agreement amongst the members of the group that the ASCII encoding of image data is not appropriate. Given that it is highly desirable that header information and the image data are kept together in the same file this means that the format is binary in nature, and cannot be considered as compliant CIF. Hence the “Not” in “imageNCIF”.

Nevertheless, the advantage of using the existing CIF structure for naming and defining data names and

definition is sufficiently important to define an associated format which is closely related to CIF: "CIF-compatible". The header section of such a file would contain CIF keyword / value pairs. This would differ from CIF in the manner in which the "lines" were separated. A simple utility program could extract the header section and write it out in a true CIF form. Similarly, analysis programs might use some of the header information for their own processing, ignore other items, and write an output CIF which contains their results plus most of the original CIF-style items. A number of new CIF data names need to be defined.

The details of this approach are presently being discussed by the working group.

### Joining "imageNCIF"

So far there are no "rules" and "imageNCIF" seems to work reasonably well on an open membership basis. I suggest that appointing one representative per institute, or one per scientific group within an institute is a sensible means by which to channel views whilst making sure that the working group does not get too big. Some input from the CCP13 community would be valuable, either through individuals or through a representative member.

### References

1.S R Hall, F H Allen, I D Brown, *Acta Cryst.*, **A47**, pp 655-685, (1991).

### Synchrotron Studies of Amyloid Fibrils

C.Blake

University of Oxford, Laboratory of Molecular Biophysics,  
South Parks Road, Oxford, OX2 9AL

Amyloid fibrils derive from the deposition of abnormal forms of normally soluble proteins in an insoluble, aggregated state in certain disease processes. Amyloid is associated with some of the most widely-publicised of modern diseases, such as Alzheimer's disease, Creutzfeldt-Jakob disease (and its animal versions Scrapie and BSE or Mad Cow's disease), Type II or late-onset diabetes, and some polyneuropathies. In most cases the diseases are chronically progressive leading inevitably to death. Each disease is associated with a specific protein which is deposited as amyloid often as the result of specific amino-acid mutation, and/or abnormal proteolytic cleavage. The amyloid most extensively

studied here is that from Familial Amyloidotic Polyneuropathy(FAP) which is composed of the protein transthyretin(TTR) in which Val30 has been substituted by Met.

In the electron microscope, amyloid fibrils have a characteristic appearance of uniform, straight, unbranched fibres about 100Å in diameter and of indefinite length. X-ray analysis of these fibrils using laboratory X-ray sources gives a relatively weak diffraction pattern, characterised by a sharp 4.8Å meridional reflection, and a more diffuse 10Å equatorial reflection, with few if any other reflections. This diffraction pattern is characteristic of the so-called cross- $\beta$  fibre structure in which the polypeptide chains in the fibril are arranged in  $\beta$ -sheets, such that the  $\beta$ -strands are perpendicular to the fibre axis, and the sheets parallel to the fibre axis. The meridional reflection then derives from the characteristic 4.8Å hydrogen-bonded separation of adjacent strands in the  $\beta$ -sheet, and the equatorial reflection from the typical  $\beta$ -sheet separation of about 10Å. Use of synchrotron radiation at Daresbury gives much more detailed diffraction patterns which can extend to at least 2.0Å along the fibre axis and to about 3.5Å perpendicular to the fibre axis. However, difficulties with orientation of the long fibrils from disease state amyloid prevents the development of reflections other than meridionals and equatorials. In spite of this limitation 7 clear meridional reflections can be detected on the synchrotron pattern, which can be indexed precisely to an axial repeat of 115.5Å. The tendency for the indices of the stronger meridional reflections to be divisible by 3 indicates the presence of a (pseudo) three-fold screw axis parallel to the fibre axis.

Interpretation of the synchrotron X-ray patterns is based on the observation that the intense 4.8Å meridional is the 24th. order of the 115.5Å cell, indicating that the axial repeat corresponds to a group of 24  $\beta$ -strands which the three-fold screw axis divides into three sets of eight. As the TTR molecule is composed of four  $\beta$ -sheets each containing eight  $\beta$ -strands it is possible, though not necessary, for the cell to contain three TTR molecules. In any event a "standard" 8-stranded  $\beta$ -sheet will be 38.5Å wide and its  $\beta$ -strands will twist through 120°, and thus when operated on by a three-fold screw axis will generate a 24-stranded  $\beta$ -sheet 115.5Å long whose 0th. and 24th. strands are twisted through 360°. On this basis the repeat unit in the amyloid fibril corresponds to one turn of a  $\beta$ -sheet helix containing 24  $\beta$ -strands. This new

description of the molecular structure of the amyloid fibril reconciles the classical description of it as a cross- $\beta$  structure with the twisted  $\beta$ -sheet now known to be the lowest energy state, and in doing so generates a new fibrous protein structure in which  $\beta$ -strands can be hydrogen-bonded together over large distances in a stable structure.

### Time-Resolved SAXS Measurements on Gel Setting and Gel Melting of Triblock Copolymer Gels

K. Reynders, H. Reynaers

Laboratory of Macromolecular Chemistry, Catholic University of Leuven, Celestijnlaan 200 F, B-3001 Heverlee, Belgium

The unique properties and practical applications of triblock copolymer gels are related to the specific morphology. The endblocks of a triblock copolymer, polystyrene-block-(hydrogenated butadiene)-block-polystyrene (SEBS) or polystyrene-block-(hydrogenated isoprene)-block-polystyrene (SEPS), will associate in a solvent selective for the midblock, and result in a three-dimensional organisation. This implies an electron density difference, detectable in a small-angle scattering experiment, if the superstructure has dimensions in the range of 10 - 1000 Å.

The gels were investigated by small-angle scattering of X-rays and neutrons (SAXS and SANS) and exhibit a pronounced superstructure[1] which appears to be a function of the block copolymer concentration, molar mass, end/mid block ratio, deformation [2] and temperature. From the variations in the two interdomain interference maxima and one or more intradomain interferences with varying sample parameters, it follows [3] that the polymer concentration and molar mass influence the degree of organisation in the gel. A certain molar mass corresponds, for a specific polymer concentration, to the most disordered arrangement. Each deviation from these values introduces more order. The scattering patterns of the isotropic samples are fitted with two different models [3]; the Percus-Yevick hard-sphere interacting liquid model and the local coordination model of distorted hexagonal lattice.

Recent time-resolved SAXS experiments [4] reveal changes in the superstructure. Upon heating, the morphological order disappears, in agreement with DSC and rheological experiments. Gels with high molar mass, show a initial increase in order. These gels reach a thermodynamically more favourable morphology. After heating these gels with high block

molar mass above the temperature where disordering occurs, followed by cooling, they again exhibit increased order. Thermo-reversibility appears for these gels after a second heating scan.

Another effect is the temporarily change in structure for gels with relatively low block molar mass from hexagonal to a cubic-like order at a temperature around 120°C. Isothermal SAXS experiments in a temperature region around 100°C, reveal the same changes in superstructure. These morphological changes involve chain mobility which is relatively low in the case of long chain lengths. This explains the temperature difference, related to a time-effect, between dynamic and isothermal SAXS measurements. These morphological changes correspond to a critical gel formation in rheology experiments [5], performed in the same temperature region.

In the case where no improvement of order occurs during heating, cooling the gel from the temperature where the gel is in the disordered state yields the same scattering curve as before heating, indicating their thermo-reversibility.

### References

1. N.Mischenko, K.Reynders, K.Mortensen, R.Scherrenberg, F.Fontaine, R.Graulus, H.Reynaers. *Macromolecules*, **27**, 2345-2347 (1994)
2. K.Reynders, N.Mischenko, K.Mortensen, N.Overbergh, H.Reynaers. accepted for *Macromolecules*
3. N.Mischenko, K.Reynders, M.H.J.Koch, K.Mortensen, J.S.Pedersen, F.Fontaine, R.Graulus, H.Reynaers. *Macromolecules*, **28**, 205-2062 (1995)
4. K.Reynders, M.H.J.Koch, N.Mischenko, H.Soenen, H.Reynaers. To be published in *Macromolecules*.
5. H.Soenen, A.Liskova, K.Reynders, H.H.Winter, H.Berghmans submitted to *Macromolecules*.

# Small Angle Scattering of Biological and Polymer Samples under Pressure at the ESRF.

M. Lorenzen

European Synchrotron Radiation Facility (ESRF), B.P. 220, F-38043 Grenoble Cedex, France

## Introduction

Small-angle scattering under pressure has been done up to now only with neutrons [1] because existing X-ray sources only deliver large cross sections of the X-ray beam with relatively low intensity. This would have led to high pressure cells with huge window apertures and, thus, thick windows and high absorption. These difficulties can be overcome with third generation synchrotron sources that deliver an X-ray beam of high brilliance. At the ESRF, we constructed a high pressure cell and used it for different types of samples. A short overview is given below.

## The high pressure cell

The high pressure cell is a large volume cell of piston cylinder type (see figure 1) [2]. Pressure is applied and controlled by an oil hand pump from outside the experimental hutch. The pump drives a movable piston through a pressure amplifier that amplifies the pressure by a factor of 64. The pressure is transmitted to the sample through a liquid so that

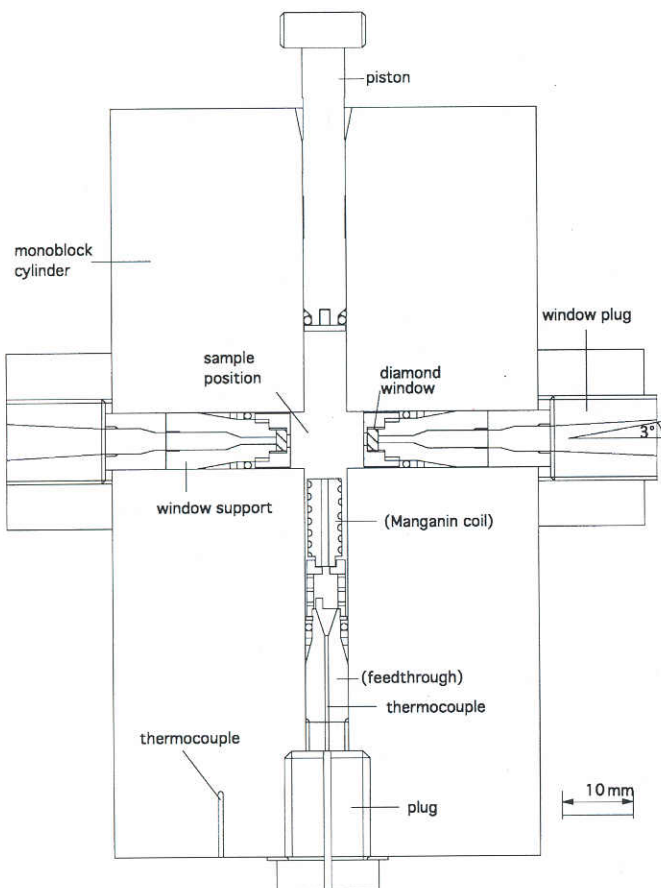


Figure 1: Schematic design of the SAXS-high pressure cell.

hydrostatic pressure conditions are ensured. Depending on the type of sample being studied, different liquids have to be used. Silicon oil, for example, is chemically inert but solidifies at elevated pressure. Diethylsebacate remains liquid throughout the whole pressure range but can react with the sample. Up to now we have used three different liquids [3]. Pressure can be increased from ambient pressure up to 1 GPa (10 kbar) and temperature from room temperature up to 300°C. The cell is heated from the outside with a heating rate of up to 3°C/min. Cooling is not yet available but is being planned.

The X-ray beam passes through the pressure cell perpendicular to the cell axis through two diamond windows of 1.5 mm thickness which have a transmission of 59% at 13 keV. The window aperture is 1 mm diameter and the maximum scattering angle is  $2\theta = 3^\circ$  for a straight incoming beam. The samples can be either solid or liquid. Solid samples can be up to 6 mm thick. They can be introduced within 15 min. Liquid samples need to be separated from the pressure transmitting liquid and they are therefore filled into Teflon containers that are squeezed between the windows. This leads to 0.2 mm of Teflon in the beam path. Therefore, the containment for liquids will be re-designed.

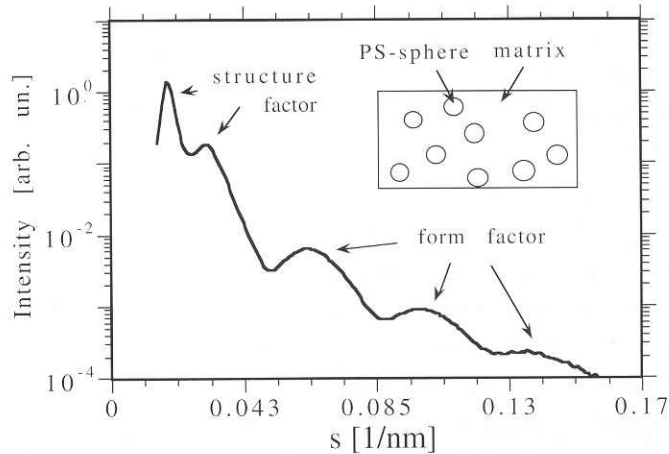


Figure 2: Small-angle scattering curve of a triblock-copolymer gel. Inset: Schematic morphology of the gel.

## Examples

### 1. Gels

Triblock-copolymer gels are studied that consist of some percent of triblock-copolymer (PS-PB/PE-PS) in an extender fluid. Their morphology has been elucidated by Mischenko et al [4]: The PS-endblocks separate from the rest (midblock + oil = matrix) and coagulate to form spheres (see inset of figure 2). This leads to small-angle scattering curves that show spherical oscillations at large s-values ('form factor')

and structural peaks at low  $s$ -values ('structure factor'). A typical curve is shown in figure 2 for a gel with 12 wt% of polymer in the sample. From the location of the oscillation maxima, the radius of the spheres can be derived; from the structural peaks, the distances between spheres can be obtained. In the example given, we will only show the pressure influence on the PS-spheres. In figure 3 the radius in relation to the pressure is given [5]. As can be seen, two regions of different slope occur: Up to 450 MPa the radius of the PS-domains decreases only slightly; above this pressure, the decrease is pronounced. This behaviour is reversible. With the help of literature data for the compressibility, the radius of the glassy PS-spheres can be calculated (for details see [3]). As can be seen in figure 3, the experimental slope below 450 MPa is lower than the calculated one whereas, above this pressure, calculation and experiment do agree well. The difference below 450 MPa can be explained by a screening effect. This could be due to an interfacial layer with a compressibility smaller than the compressibility of the matrix. So far, no proof for this idea can be given. However, there is evidence for the existence of an interfacial layer [6].

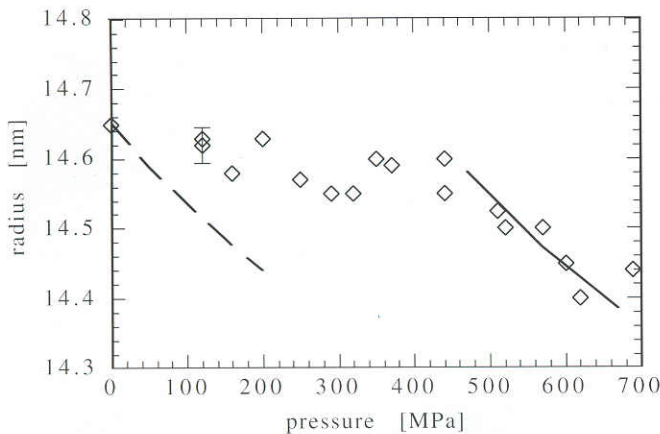


**Figure 3:** Radius of the PS-spheres as a function of pressure (diamonds: experimental data; solid and dashed line: calculations for different initial conditions).

## 2. Biological solutions

As an example for a biological solution, measurements on ATCase (Aspartic transcarbamoylase) are shown (see figure 4). As can be seen, the minimum smears out and the intensities decrease with increasing pressure. This can be interpreted as dissociation of the enzyme. According to our measurements, this behaviour is reversible.

## Conclusions

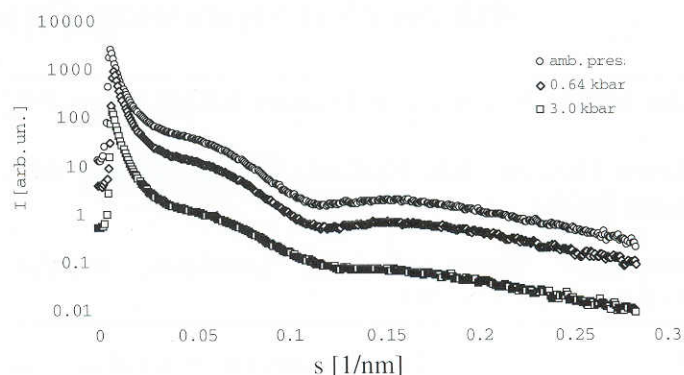


**Figure 4:** Scattering curve of ATCase as a function of pressure.

Although only a few examples are given, it can already be seen that small-angle X-ray scattering under pressure leads to interesting new results that need to be studied further. The application of pressure opens up a completely new branch of small-angle scattering studies. The high pressure cell is in use at the High Brilliance beamline (Bl#4) [7] and the Microfocus Beamline (BL#1) [8] at the ESRF. Within the usual proposal procedure at the ESRF, anybody can apply for beamtime with the high pressure cell (the proposal form can be found in WWW: <http://fox.esrf.fr:3600>).

## References

1. D. Barthels, Thesis: 'Entwicklung und Konstruktion einer Temperatur-Druck-Zelle zur Untersuchung von Polymeren mit der Neutronenkleinwinkelstreuung', Julich, 1987
2. M. Lorenzen, C. Riekel, A. Eichler, D. Hausermann, Journal de Physique IV, Colloque C8, 3 (1993) 487-490
3. M. Lorenzen, Thesis: 'Small-angle X-ray scattering of polymers under pressure', Technical University of Braunschweig, 1995
4. N. Mischenko, K. Reynders, K. Mortensen, R. Scherrenberg, F. Fontaine, R. Graulus, H. Reynaers, Macrom. 27 (1994) 2345-2347
5. M. Lorenzen, P. Bosecke, C. Riekel, K. Reynders, H. Reynaers, N. Overbergh, submitted to Makromolekulare Chemie - Rapid Communications
6. N. Mischenko, F. Fontaine, R. Graulus, H. Reynaers, Macrom. 28 (1995) 2054
7. P. Bosecke, O. Diat, B. Rasmussen, Rev. Sci. Instrum. 66 (1995) 1636
8. C. Riekel, P. Bosecke, O. Diat, M. Lorenzen, M. Sanchez del Rio, I. Snigireva, Rev. Sci. Instrum. 66 (1995) 987

## 4th Annual Workshop Prize-Winning Poster Abstracts

### An Actin's Eye View of Myosin: SAXS Meets PX

Liam Hudson, Jeff Harford, Richard Denny and John Squire

Biophysics Section, Blackett Laboratory, Imperial College, London SW7 2BZ.

Low-angle X-ray diffraction patterns from plaice fin muscle recorded on lines 2.1 and 16.1 at Daresbury (Harford and Squire, 1992) have been stripped by Richard Denny's CCP13 software (Denny, CCP13 Newsletter, 1993; 1994) to give  $h,k,l$  and intensity values as in CCP4 format. The intensities that we have modelled extend to a resolution of about 70 Å (Figure 1). Most of the observed intensity on the low-angle layer-lines is from the myosin heads that project from the surface of myosin filaments in a roughly helical array (Harford and Squire, 1986).

The structure of these heads (myosin S1) has been solved by Ivan Rayment and his colleagues (Rayment *et al.*, 1993), so the molecular shape is known. We have modelled this shape as in Figure 2; the detail is sufficient to give a transform indistinguishable from the full molecular transform at the resolution involved in our studies. Without this simplification of the head shape, our computers, although very fast, would not have been able to carry out searches and refinements in a reasonable time. Computer programs have been set up to model the observed intensities. The positions of the six non-equivalent myosin heads in the unit cell of the structure were parameterised and optimisation of an R-factor between observed and calculated intensities was obtained by simulated annealing and downhill simplex methods. The final model (Figure 3), using 56 observed independent intensities, gave an R-factor of about 3%.

The sensitivity of the modelling was tested in a number of ways and it was found that the R-factor increased very rapidly away from the preferred parameters. The preferred myosin head arrangement is

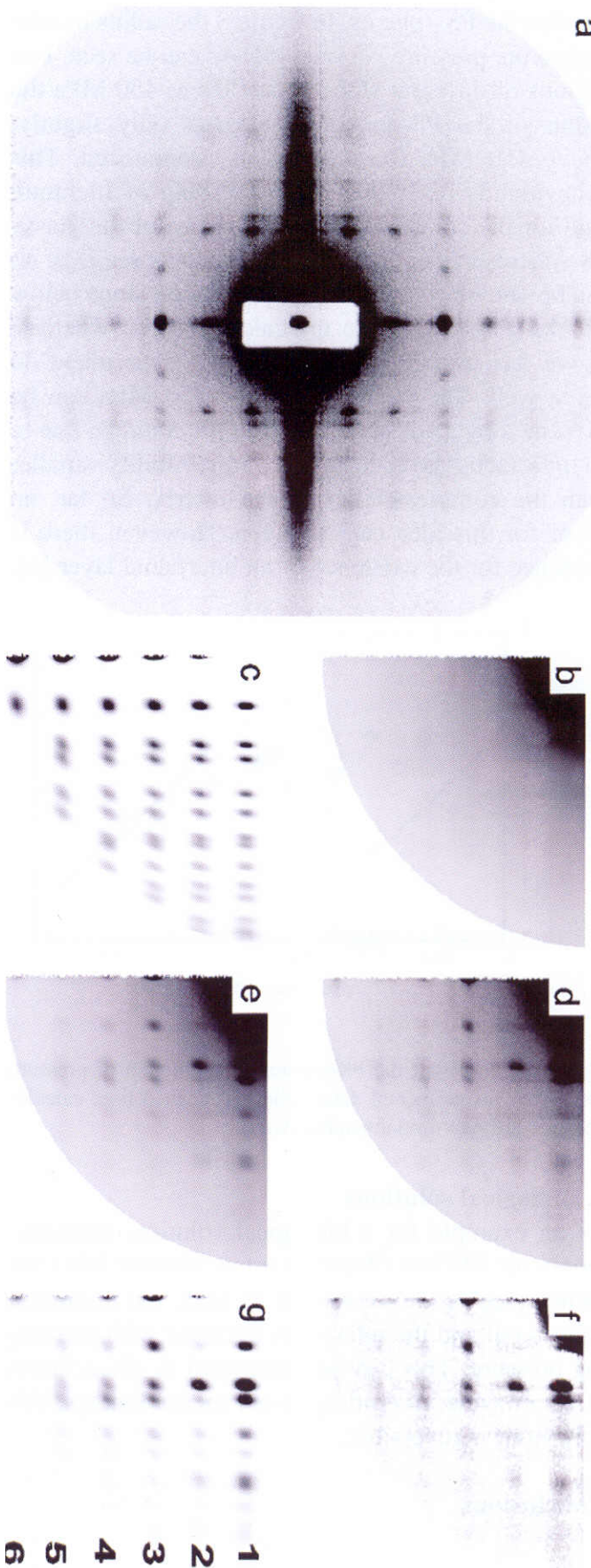


**Figure 1:** (a) Low-angle X-ray diffraction pattern from plaice fin muscle recorded on line 16.1 at the CCLRC Daresbury Synchrotron Radiation Source using a multiwire detector; fibre axis vertical, scale as in (g) which shows orders 1 to 6 of the myosin axial repeat of 429 Å. (b) to (g) Various stages in fitting of the intensities in Figure 1 using the CCP13 software packages FTOREC and LSQINT: (d) quadrant folded version of (a), (c) 'nofit' pattern showing the positions and shapes of the modelled peaks but not their relative intensities, (b) fitted background between the 'nofit' peaks, (f) observed quadrant-folded pattern (d) with the fitted background (b) removed, (g) modelled intensities of the Bragg peaks, and (e) images (b) and (g) added to simulate the whole original pattern for comparison with (d).

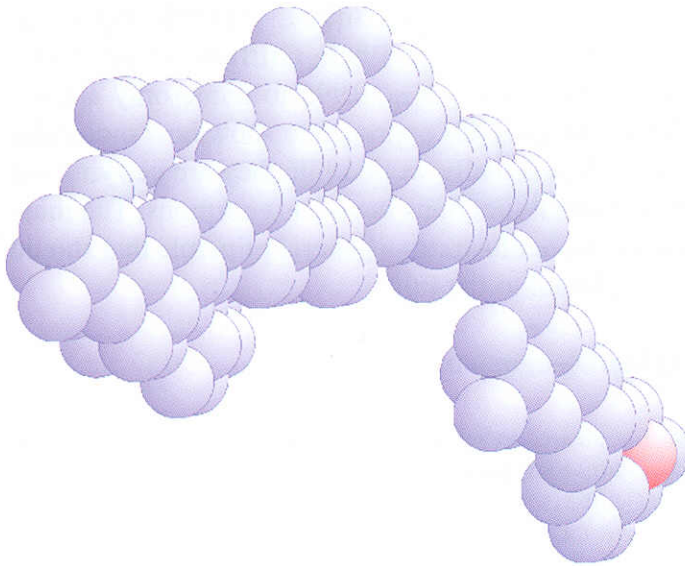


**Figure 2:** Low-resolution model of the myosin head using 59 spheres all of 7.15 Å radius. The Fourier transform of this model was tested against the original Rayment diffraction data and is indistinguishable (correlation function 0.9955) at a resolution of 65 Å.

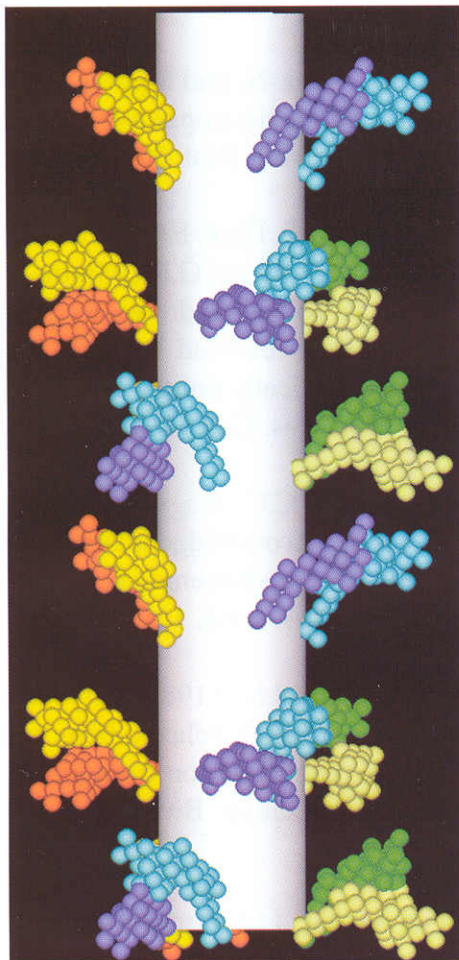


**Figure 3:** The myosin head arrangement giving the lowest R-factor (3%) after searches and optimisation using simulated annealing and downhill simplex algorithms. Note that the head arrangements on two levels are very similar, whereas that on the third is slightly different. It is known that proteins such as C-protein and titin have a 430 to 440 Å repeat along the myosin filament and these may be involved in producing this perturbation.

probably accurate to a few Å, even though only low-angle data are being used. This is because a considerable amount of high resolution knowledge about the protein structure is being included in the modelling. For example, changes in tilt (towards the filament long axis), slew (around the filament long axis) or rotation of the myosin heads about their own long axis of  $\pm 5^\circ$  roughly doubled the R-factor.

The goodness of fit was also very dependent on the absolute rotation of the filament around its long axis within the muscle A-band unit cell. The relative positions of the myosin heads and actin filaments in resting fish muscle have therefore been defined. By identifying the actin binding sites on the myosin heads, the locations of these relative to actin can also be determined. The result is shown in Figure 4, which illustrates the fish muscle A-band unit cell

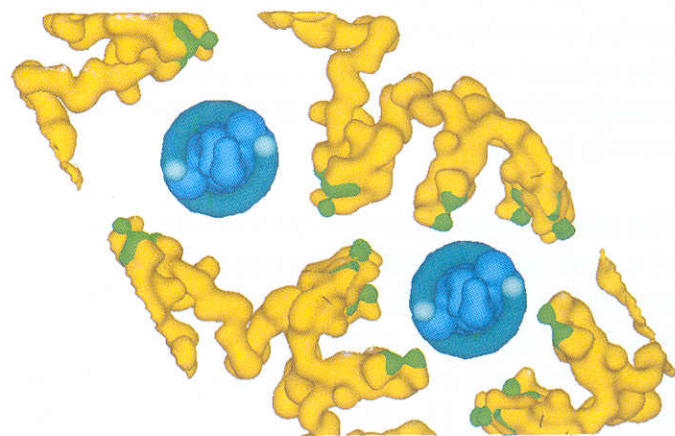


**Figure 4:** View of the fish muscle A-band unit cell looking down the muscle long axis and showing the arrangement of myosin heads around the two actin filaments. The actin-binding sites on the heads are highlighted (green) and can be seen to be facing the actin filaments (unit cell side is about 470 Å).

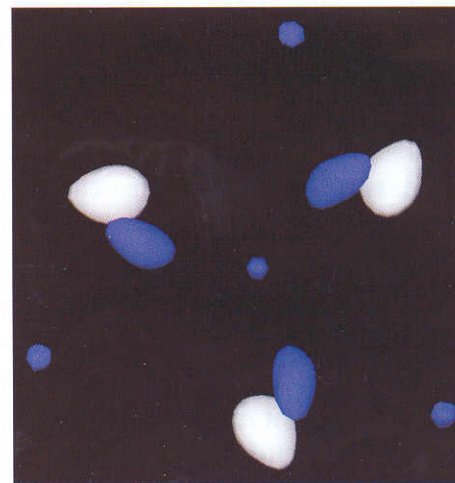


**Figure 5:** Fourier difference map obtained by modelling two structures, the preferred head arrangement in Figure 3 and the same structure with one of the six non-equivalent heads moved out of position. The Fourier difference synthesis from these two structures at 70 Å resolution clearly shows negative and positive density peaks related to the single head movement.

containing one myosin filament and two actin filaments. The actin binding sites on the myosin heads are very close to and facing their target binding sites on the neighbouring actin filaments.

One of the postulated mechanisms for the generation of force and movement in muscle is that once bound to actin the myosin heads undergo an ATP-driven change in their shape by bending about halfway along their length to move the myosin end of the head axially relative to the actin-bound end. The potential for bending in the head was tested in the relaxed state in our modelling by including two head bend angles in the parameter search. The calculated R-factor was also very sensitive to these two angles and the best model had these head bend angles almost precisely as in the original myosin S1 structure of Rayment *et al* (1993). This shape seems also to be very close to the shape at the end of the power stroke, assuming it is like the rigor state in muscle. The relaxed structure is therefore already providing considerable insights into the possible mechanism of myosin head action.

The relaxed state diffraction pattern is the first frame of a time series of diffraction patterns at 5 ms time resolution. The idea is to bootstrap our way through this time series by modelling based on the first frame. This will generate a series of images to produce "Muscle - The Movie" (Squire *et al*, 1993). Fourier difference synthesis will be helpful in generating this movie. We have tested the potential of this by modelling two structures, one our best relaxed structure, as above, and the other the same structure with just one of the six non-equivalent myosin heads moved out of position. Even at 70 Å resolution, the movement of this one head is readily detectable by Fourier difference synthesis (Figure 5).

These various results serve to illustrate a number of important points with regard to what can be achieved with low-angle diffraction data that has been properly stripped by appropriate software (e.g. the CCP13 package) and has been carefully modelled using proteins of known structure. We have previously published analysis of actin filament structure using related methods (AL-Khayat *et al*, 1995), and the current analysis of the myosin head array reinforces the view that highly accurate modelling with positional sensitivities of a few Å can be achieved from low-resolution X-ray diffraction data. Since techniques are already available for carrying out time-resolved low-angle X-ray diffraction experiments (e.g. Huxley *et*

*al*, 1983; Harford and Squire, 1992; Irving *et al*, 1992; Bordas *et al*, 1993; Griffiths *et al*, 1993; Martin-Fernandez *et al*, 1995 to name only a few), the potential of this approach to show how molecular assemblies actually work while they are carrying out their normal functions *in vivo* is enormous. The muscle example illustrates a general principle that should be exploited to the full.

## Acknowledgements

We are pleased to acknowledge the help of many people at the Daresbury SRS, particularly Liz Towns-Andrews, Sue Slawson and Geoff Mant for practical help with stations 2.1 and 16.1 and the detector group, especially Rob Lewis and Chris Hall, for their excellent area detectors. This work is funded mainly by the BBSRC (project grants #28/S02028 and #28/X04460) and by the MRC which provides a studentship for LH. We are also indebted to our colleagues Michael Chew, Ed Morris and John Barry for various discussions and to Peter Brick's crystallography group for help with molecular graphics.

## References

- AL-Khayat, H.A., Yagi, N. and Squire, J.M. (1995) Structural changes in actin-tropomyosin during muscle regulation. *J. Mol. Biol.* **252**, 611-632.
- Bordas, J., Diakun, G.P., Diaz, F.G., Harries, J.E., Lewis, R.A., Lowy, J., Mant, G.R., Martin-Fernandez, M.L. & Towns-Andrews, E. (1993) Two-dimensional time-resolved X-ray diffraction studies of live isometrically contracting frog sartorius muscle. *J. Mus. Res. Cell Motil.* **14**, 311-324.
- Griffiths, P.J., Ashley, C.C., Bagni, M.A., Maeda, Y. & Cecchi, G. (1993) Crossbridge attachment and stiffness during isotonic shortening of intact single muscle fibres. *Biophys. J.* **64**, 1150-1160.
- Harford, J.J. & Squire, J.M. (1986) 'Crystalline' myosin crossbridge array in relaxed bony fish muscle: Low-angle X-ray diffraction from plaice fin muscle and its interpretation. *Biophys. J.* **50**, 145-155.
- Harford, J.J. & Squire, J.M. (1992) Evidence for structurally different attached states of myosin crossbridges on actin during contraction of fish muscle. *Biophys. J.* **63**, 387-396.
- Huxley, H.E., Simmons, R.M., Faruqi, A.R., Kress, M., Bordas, J. & Koch, M.H.J. (1983) Changes in the X-ray reflections from contracting muscle during rapid mechanical transients and their structural

implications. *J. Mol. Biol.* **169**, 469-506.

Irving, M., Lombardi, V., Piazzesi, G. & Ferenczi, M.A. (1992) Myosin head movements are synchronous with the elementary force-generating process in muscle. *Nature* **357**, 156-158.

Martin-Fernandez, M.L., Bordas, J., Diakun, G., Harries, J., Lowy, J., Mant, G.R., Svensson, A. & Towns-Andrews, E. (1994) Time-resolved X-ray diffraction studies of myosin head movements in live frog sartorius muscle during isometric and isotonic contractions. *J. Mus. Res. Cell Motil.* **15**, 319-348.

Rayment, I., Rypniewski, W.R., Schmidt-Base, K., Smith, R., Tomchick, D.R., Benning, M.M., Winkelmann, D.A., Wesenberg, G. & Holden, H.M. (1993a) Three-dimensional structure of myosin subfragment-1: a molecular motor. *Science* **261**, 50-58.

Squire, J.M., Harford, J.J. and Morris, E.P. (1993) Muscle - the Movie. In *Image Processing*, Spring 1993, pp. 22, 23. Reed Publishing Group.

### Simultaneous SAXS/FT-IR Studies of Reaction Kinetics and Structure Development During Polymer Processing

A. J. Ryan, J. Cooke, M.J. Elwell, P. Draper, S. Naylor, D. Bogg<sup>1</sup>, G. Derbyshire<sup>1</sup>, B.U. Komanschek<sup>1</sup> and W. Bras<sup>2</sup>

Manchester Materials Science Centre, UMIST

<sup>1</sup>CCLRC, Daresbury Laboratory

<sup>2</sup>AMOLF, The Hague, The Netherlands

In a novel combination, synchrotron radiation small angle X-ray scattering (SAXS) and Fourier Transform infra-red spectroscopy (FT-IR) experiments have been performed on a series of model segmented polyurethanes [1]. This combination of techniques is potentially a very powerful research tool, not only for polymer research, but for a wide variety of research fields including biological gel formation, food processing and conformational changes in proteins.

The major theme of the research group's work is studying the *in-situ* development of structure during the processing of multiphase polymers, in particular polyurethanes [1-6]. These materials are of great

commercial utility combining unique mechanical properties with ease of processing. Polyurethanes are formed by the reaction between a diisocyanate, a short chain diol and a macroglycol. The development of polymer morphology is complex [1,4] and the process can be best described as a reaction-induced phase separation. The morphology formed is determined by the kinetic competition between polymerization and microphase separation [5]

The experimental configuration, methods and chemical systems studied are described in detail elsewhere [1]. FT-IR spectroscopy is used to monitor the reaction chemistry and SAXS is used to monitor the development of polymer morphology on the sizescale of 20-1000 Å. Figure 1 shows the decay in the isocyanate absorbance (which correlates with the polymerization kinetics) and the growth in the carbonyl absorbances [1,6]. Figure 2 shows the SAXS data, which indicate the development of polymer structure with a length scale of ≈ 118 Å. Figure 3 shows the onset of microphase separation detected by both SAXS and FT-IR. Microphase separation precedes hydrogen bonding and is driven by the free energy of mixing. This causes the groups that are capable of hydrogen bonding to achieve a locally high concentration and their rate of association increases. The hydrogen bonding is thus parasitic and *not* the driving force.

### References

1. Bras, W.; Derbyshire, G.E.; Bogg, D.; Cooke, J.; Elwell, M.J.; Komanschek, B.U.; Naylor, S. and Ryan, A.J. *Science*, **1995**, 267, 996.
2. Ryan, A.J.; Stanford, J.L. and Tao, X.Q. *Polymer*, **1993**, 34, 4020.
3. Ryan, A.J.; Macosko, C.W. and Bras, W. *Macromolecules*, **1992**, 25, 6277.
4. Elwell, M.J.; Mortimer, S. and Ryan, A.J. *Macromolecules*, **1994**, 27, 5428.
5. Ryan, A.J. *Polymer*, **1990**, 31, 707.
6. Elwell, M.J. Ph.D. Thesis, Victoria University of Manchester **1993**.

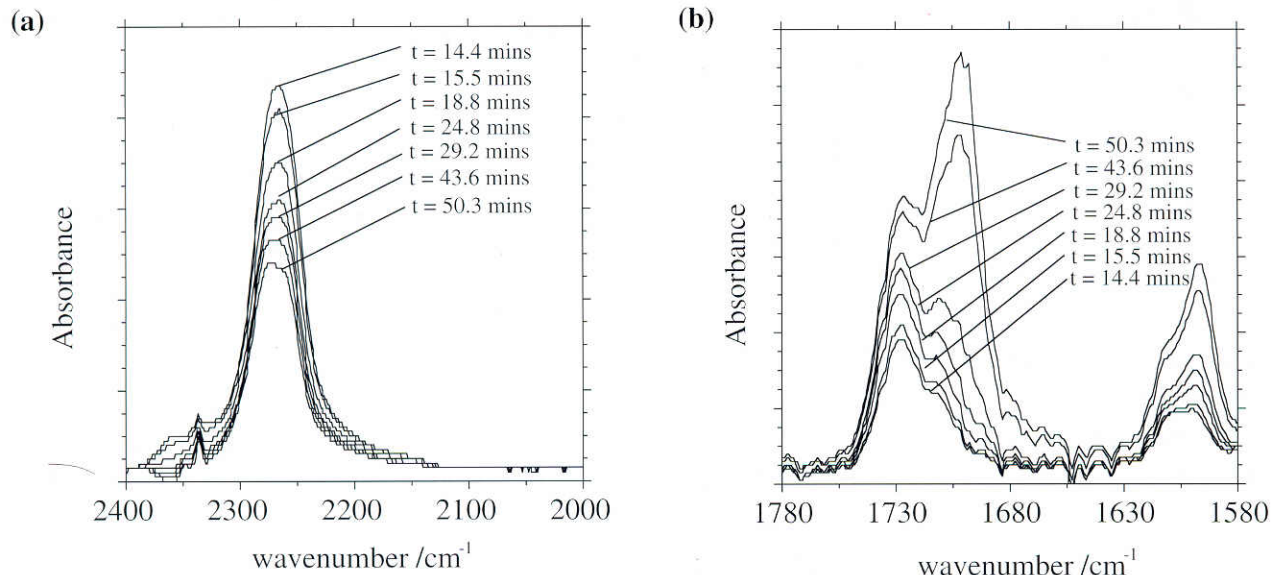


**Figure 1.**

(a) Absorbance versus frequency illustrating the decay in the intensity of the isocyanate absorbance ( $\approx 2270 \text{ cm}^{-1}$ ) at selected times for a model segmented block copolyurethane at  $35 \pm 1 \text{ }^{\circ}\text{C}$ . (b) Absorbance versus frequency illustrating the carbonyl region of the mid-infrared spectrum, at selected time frames for the same model segmented block copolyurethane at  $35 \pm 1 \text{ }^{\circ}\text{C}$ .

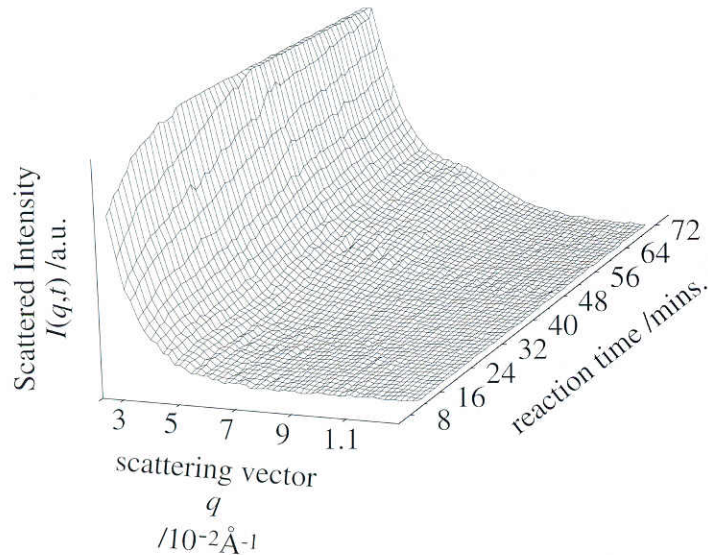
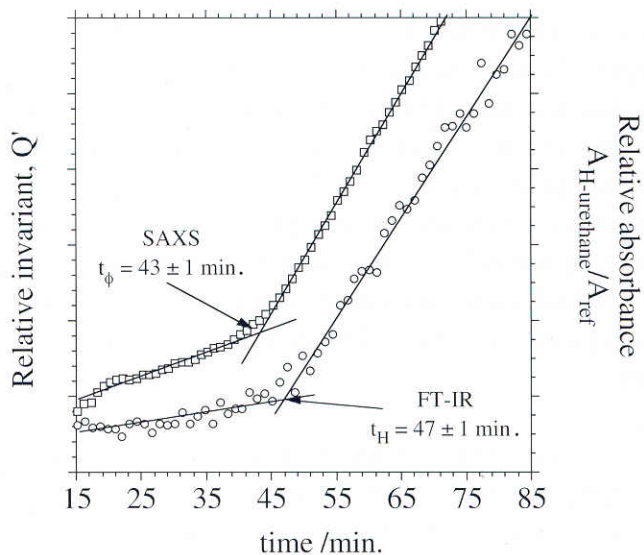


**Figure 2.**

The time evolution of the SAXS pattern is illustrated as a time-stack of the scattered intensity,  $I(q,t)$ , versus scattering vector,  $q$ . The data were recorded in frames of 60 s. For clarity, only every fourth frame of data is shown. Initially there is little scattering and the peak that starts to grow at  $q = 0.053 \text{ \AA}^{-1}$  after  $\approx 40$  minutes is evidence for the structural development in the material with a linear dimension of  $\approx 118 \text{ \AA}$ .

**Figure 3.**

The SAXS relative invariant,  $Q' = \int I(q,t)q^2 dq$  and the normalised FT-IR absorbance associated with hydrogen-bonded urethane are plotted against time, for a model segmented block copolyurethane investigated at  $25 \pm 1 \text{ }^{\circ}\text{C}$ . Tangents have been fitted to both data sets in order to estimate the onset times for microphase separation ( $t_{\phi}$ ) and hydrogen bonding ( $t_H$ ). The values of  $t_{\phi}$  and  $t_H$  are  $43 \pm 1$  and  $47 \pm 1$  minutes respectively. The perfect time correlation between the two techniques confirms unambiguously that microphase separation precedes hydrogen bonding in the reactive processing of this polyurethane block copolymer.



## 4th Annual Workshop Abstracts

### Synchrotron X-ray and Neutron Solution Scattering Studies of the Complex Formed Between the Extracellular Domain of Human Tissue Factor and Factor VIIa

A.W. Ashton<sup>1</sup>, D.J.D. Johnson<sup>2</sup>, D.M.A. Martin<sup>2</sup>, D.P. O'Brien<sup>2</sup>, G. Kemball-Cook<sup>2</sup>, E.G.D. Tudenham<sup>2</sup> and S.J. Perkins<sup>1</sup>

<sup>1</sup>Department of Biochemistry and Molecular Biology, Royal Free Hospital School of Medicine, Roland Hill Street, London NW3 2PF

<sup>2</sup>Haemostasis Research Group, MRC Clinical Sciences Centre, Royal Postgraduate Medical School, Du Cane Road, London W12 0NN

Blood coagulation has long been recognised as an important process essential for survival. Exposure of the membrane-bound receptor tissue factor to plasma initiates the coagulation pathways. The four domain structure of human factor VIIa and the two domain structure of tissue factor form a very stable enzyme-cofactor complex. In order to elucidate the arrangement of these domains in complex formation, the two soluble recombinant proteins were studied by synchrotron X-ray and pulsed neutron scattering (in 100% <sup>2</sup>H<sub>2</sub>O buffer). The X-ray and neutron radii of gyration R<sub>G</sub> were determined to be close to 3.3 nm (factor VIIa), 2.1 nm (extracellular tissue factor) and 3.1 nm for their complex. The neutron cross sectional radii of gyration R<sub>xs</sub> were 1.1 nm, 0.6 nm and 1.3 nm in that order. Calculation of the distance distribution function P(r) curves gave maximum dimension of 10 nm, 8 nm and 10 nm in that order. The data show that both proteins have extended structures in solution, which associate side-by-side along their long axes to form the complex. A crystal structure is known for tissue factor, and crystal or NMR structures are known for domains homologous to those of factor VIIa. Using a newly-developed automated computerised search-and-evaluation technique, along with biochemical evidence relating to residues known to lie at the interface between tissue factor and factor VIIa, we are modelling the structures of the free proteins and their complex. We hope to derive insight into the structure of the complex, and obtain an enhanced understanding of how specific residues contribute to complex formation.

### Thermotropic Cubic Phases Formed by Cone-Shaped Molecules

V.S.K. Balagurusamy<sup>1</sup>, G. Ungar<sup>1</sup>, D. Abramic<sup>1</sup>, V. Percec<sup>2</sup> and J. Heck<sup>2</sup>

<sup>1</sup>Department of Engineering Materials and Centre for Molecular Materials, University of Sheffield S1 4DU

<sup>2</sup>Department of Macromolecular Science, Case Western Reserve University, Cleveland USA

X-ray diffraction experiments of the three derivatives of cone-shaped 3,4,5-tris[3,4,5-tris(dodecyl-1-yloxy)benzyloxy] benzoic acid (**ABG-COOH**) confirmed the formation of a cubic liquid crystalline phase. Powder diffraction data combined with the diffraction patterns of monodomains suggest that the molecules are clustered around special positions of the space-group Pm $\overline{3}$ n. We have computed the electron density using the very intense reflections. These results and their implication for the molecular organisation will be presented. The suggested model is different from that proposed for the micellar lyotropic Pm $\overline{3}$ n phase[1,2] which forms in some lipids.

### References

1. K. Fontell, K.K. Fox and E. Hansson 1985 Mol.Cryst.Liq.Cryst. **19**
2. V. Luzzati, R. Vargas, P. Mariani, A. Gulik and H. Delacroix 1993 J.Mol.Biol. **229** 540

### Automated Modelling of the Multidomain Structure of Carcinoembryonic Antigen

Mark K. Boehm<sup>1,2</sup>, M. Olga Mayans<sup>1</sup>, Jeremy R. Thornton<sup>2</sup>, Pat A. Keep<sup>2</sup>, Richard H. J. Begent<sup>2</sup> and Stephen J. Perkins<sup>1</sup>

<sup>1</sup>Departments of Biochemistry and Molecular Biology, and

<sup>2</sup>Clinical Oncology, Royal Free Hospital School of Medicine, Rowland Hill Street, London NW3 2PF, U.K.

Carcinoembryonic antigen (CEA) is a cell-surface glycoprotein that is involved in the detection of colonic tumours through the generation of anti-CEA antibodies. Its amino acid sequence reveals that it consists of a single V-type and six C2-type domains in the immunoglobulin superfamily, together with 28 putative N-linked glycosylation sites. X-ray and neutron scattering studies on solubilised CEA have been used to determine the structural arrangements of its seven domains. The radii of gyration R<sub>G</sub> of CEA were determined in Guinier analyses to be 8.0-8.8 nm by

X-rays using H<sub>2</sub>O buffers and neutrons using 100% D<sub>2</sub>O buffers. The cross-sectional radii of gyration R<sub>xs</sub> were 2.1- 2.3 nm by X-ray and neutrons. These results indicate that CEA has an elongated structure with large cross-sectional dimensions. Molecular models of CEA were constructed from atomic coordinates. Sequence comparisons of CEA with the homologous proteins CD2 and CD4, for which crystal structures are available, show that the peptides which link the seven CEA domains are similar in length to those found in the CD2 crystal structures. The human CD2 crystal structure consists of a V-type and a C2-type domain, and was used to model the seven CEA domains. An atomic model of an averaged carbohydrate structure was constructed and 28 were added to the CEA model at each position to correspond to the glycosylation sites. Two-density sphere models were generated for X-ray and neutron curve simulations. An automated computer search procedure explored the arrangement of the seven glycosylated domains in CEA by generating a representative range of structures, and testing the scattering curves calculated from these against the X-ray and neutron data. The models which best satisfied the experimental data have domains which are twisted and tilted relative to their neighbouring domains in an orientation that is similar to the conformations of domain pairs observed in the crystal structure of CD2. The carbohydrate chains were found to have extended conformations in order for the CEA models to satisfy the experimental data. The gross morphology of the best models are analogous to the rod-shaped molecules observed by electron microscopy. This model may provide insight on the interaction of CEA domains with anti-CEA antibodies.

### Magnetic Alignment of Microtubules

W.Bras<sup>1</sup>, G.Diakun<sup>2</sup>, R.Denny<sup>2</sup>, H.Kramer<sup>3</sup>, F.Diaz<sup>4</sup> and J.Bordas<sup>5</sup>.

<sup>1</sup>AMOLF/NWO

<sup>2</sup>Daresbury Laboratory.

<sup>3</sup>Grenoble High Magnetic Field Laboratory.

<sup>4</sup>Leuven University.

<sup>5</sup>Liverpool University.

Several attempts to obtain high resolution X-ray fibre diffraction patterns of microtubules can be found in the literature. The main problem so far has been to obtain highly aligned samples of microtubules of which the structure was not altered in a significant way either through dehydration, mechanical or radiation damage.

For suitable diamagnetic macromolecules it is possible to use high magnetic fields to prepare an aligned sample. We have applied this alignment method to microtubules. The dynamic behaviour of the microtubules in the magnetic field has been studied with magnetic birefringence. Some of these results will be discussed. Also the results of X-fibre diffraction experiments will be shown.

### CCP13 Program Developments

R.C. Denny

Biophysics Section, Blackett Laboratory, Imperial College, London SW7 2BZ and  
CLRC Daresbury Laboratory, Warrington, Cheshire WA4 4AD

Modifications made to existing CCP13 programs and some new programs will be described. The 2-D background and peak fitting program LSQINT has been modified to cope with the presence of intensity from multiple lattices on a single diffraction pattern. FIX has been modified to enable simultaneous refinement of pattern centre, rotation and specimen tilt parameters. A prototype program TBACK has been written which fits the central broad background peak which is present in many diffraction muscle patterns. This is done by utilizing a penalty function which ensures the fitted peak does not cut through desired signal. A routine, SAMPLE, to smooth noisy continuous layer line intensity using the Fourier-Bessel interpolation formula given by Makowski (1982) has also been included in the suite. Attempts at producing a practical routine for deconvoluting the main beam profile from small angle diffraction patterns will also be discussed.

### References

1. Makowski, L. (1982). *J. Appl. Cryst.* **15** 546 557

### Simultaneous X-ray & Optical Techniques in Liquid Crystals & Polymeric Systems

G K Bryant<sup>1</sup>, A Morse<sup>1</sup>, H F Gleeson<sup>1</sup>, A J Ryan<sup>2</sup>, W Bras<sup>3</sup> and B Komanschek<sup>4</sup>

<sup>1</sup>Dept. of Physics & Astronomy, University of Manchester.

<sup>2</sup>Materials Science Centre, UMIST.

<sup>3</sup>Netherlands Organisation for Scientific Research.

<sup>4</sup>Daresbury Lab., Warrington.

Concurrent experiments involving synchrotron radiation offer detailed and accurate information on a minimal time scale. In the study of liquid crystal devices and polymeric systems two key measurements are X-ray scattering and optical/electro-optical

responses. This paper describes novel apparatus[1] allowing:

(i) The simultaneous observation of time dependent small angle X-ray scattering and birefringence changes of liquid crystal devices. This apparatus is incorporated into the X-ray system at station 2.1, Daresbury Laboratory.

(ii) The simultaneous measurement of time resolved small angle and wide angle X-ray scattering with Raman spectroscopy. This apparatus was designed to operate at station 8.2, Daresbury Laboratory.

Electro-optic responses are determined using a specially mounted diode laser and photodiode detector, a hot stage and temperature controller are also incorporated into the apparatus to allow the study of liquid crystal devices. The Raman spectrometer is mounted in a unique geometry defined by the space available and includes an air cooled Argon Ion laser and a high resolution monochromator. Both sets of apparatus are described in detail and simultaneous acquired results are presented.

## References

1. H F Gleeson, C Carboni & A Morse, Rev. Sci. Inst., *In Press*.

### Conformations of AMIC, the Amide Sensor Protein of *Pseudomonas Aeruginosa*: A Preliminary Study with SAXS and SANS

D. Chamberlain<sup>1</sup>, B. O'Hara<sup>2</sup>, S. A. Wilson<sup>2</sup> and S. J. Perkins<sup>1</sup>

<sup>1</sup>Royal Free Hospital School of Medicine, Department of Biochemistry and Molecular Biology, Rowland Hill Street, London NW3 2PF.

<sup>2</sup>Dept. of Biochemistry and Molecular Biology, University College London, Gower Street, London WC1E 6BT

The amidase operon consists of 5 genes, *amiE*, *amiB*, *amiC*, *amiR*, and *amiS*, and is involved with amide metabolism in bacteria. AmiC is the amide sensor protein, and is the negative regulator of the amidase operon. The crystal structure of AmiC shows that the overall fold of AmiC is very similar to that found in the crystal structure of the leucine-isoleucine-valine binding protein (LivJ) of *Escherichia coli*, despite only a 17% amino acid sequence identity. AmiC has two domains, which interestingly are in a substantially closed conformation, compared to an open one seen in LivJ. The AmiC amide binding site is extremely specific for acetamide, and the anti-inducer molecule butyramide ( $\text{CH}_3\text{CH}_2\text{CH}_2\text{CO.NH}_2$ ) binds 100-fold more weakly to AmiC than acetamide ( $\text{CH}_3\text{CO.NH}_2$ ). To test whether AmiC has different

domain structures with acetamide and butyramide, the two forms were studied by both neutron and X-ray scattering. The neutron and X-ray radii of gyration  $R_g$  values were each in good agreement with each other for both forms. Values close to 3.2 nm for neutrons in 100%  $^2\text{H}_2\text{O}$  and 3.4 nm for X-rays were obtained under conditions where the molecular weight of AmiC was shown to be similar from the  $I(0)/c$  values. These data suggest that if there is a conformational change it is too small to influence the observed  $R_g$  values. AmiC is normally thought to be dimeric. Despite this, we have X-ray data which corresponds to AmiC monomers. From these, a good curve fit could be obtained by calculation from the monomeric "closed" AmiC coordinates, which is distinct from that for the "open" LivJ crystal structure. Other X-ray data correspond to AmiC dimers, and these give good agreement with the curve calculated from the crystal structure of dimeric AmiC. At higher AmiC concentrations, the scattering curves change again to a putative trimeric or tetrameric form. Gel filtration experiments suggest however that only the dimeric form is present. These anomalies are under further investigation. At present, it can be concluded that for similar oligomeric forms in AmiC, no conformational changes between the acetamide-bound and butyramide-bound forms can be detected.

### Simultaneous SAXS/WAXS/DSC Studies of Linear and Cyclic Poly(ethylene oxide)

Jennifer Cooke<sup>1</sup>, Anthony J. Ryan<sup>2</sup>, Tao Sun<sup>3</sup>, Ga-Er Yu<sup>3</sup> and Colin Booth<sup>3</sup>

<sup>1</sup>Manchester Materials Science Centre, UMIST, Grosvenor Street, Manchester, M1 7HS

<sup>2</sup>Daresbury Laboratory, Warrington, Cheshire, WA4 4AD

<sup>3</sup>Manchester Polymer Centre, Department of Chemistry, University of Manchester, Manchester, M13 9PL

The crystallisation behaviour of several poly(ethylene oxide) samples has been studied using DSC, hot-stage optical microscopy and a time-resolved SAXS/WAXS/DSC technique developed at Daresbury Laboratory. Linear PEO molecules with nominal molecular weights ( $\bar{M}_n$ ) of 1500, 2000 and 3000 have been produced for this study, some of which were then cyclised using an acetal condensation, to give cyclic molecules [1,2].

Simultaneous SAXS/WAXS patterns were obtained from rings of molecular weight 2000, 3000, 4000, and 10000 and the 1500, 2000, and 3000 linear molecules during melting and recrystallisation. While the wide-angle patterns confirm the same helical

structure is present for each of the samples, it has been observed experimentally from the SAXS patterns that the long spacings of linear molecules are double those of the corresponding molecular weight cyclic samples. In addition, during heating of the 3000 and 10000 rings below their melting points, first order peaks in  $Iq^2$  from the small-angle patterns, have been observed to shift to a lower value of  $q$  which is consistent with a doubling of the long spacing. This change has been attributed to the unfolding of the molecules, that is, that the sample originally contained folded molecules which were able to unfold on heating.

## References

1. J. Cooke, A.J. Ryan, Tao Sun, Ga-Er Yu and C. Booth, Submitted to *Polym. Commun.*, March 1995.
2. K. Viras, Ze-Gui Yan, C. Price, C. Booth and A.J. Ryan, *Macromolecules*, **28**, 104 (1995)

## Using Synchrotron Radiation to Examine the *in-situ* Processing of Long-Chain Hydrocarbons

Richard van Gelder<sup>1</sup>, Kevin J Roberts<sup>1</sup> and Alessandra Rossi<sup>1</sup>

<sup>1</sup>Department of Pure and Applied Chemistry, University of Strathclyde, Glasgow G1 1XL; in collaboration with M Polgreen, M Wells, Cadbury Ltd; I Smith, Reading Scientific Services; T Instone, J Chambers, Unilever Research

With support from the EPSRC Structured Materials Initiative, Cadbury Ltd and Unilever Research we are involved in two parallel investigations:

- In order to elucidate the crystallisation behaviour of cocoa butter, which is the main ingredient of chocolate we want to characterise the polymorphic structures and phase transitions of fat systems. In chocolate manufacturing, careful control of the solidification processes is quite important because it significantly influences both rheological and physical properties of end products.
- Processing and in-use behaviour of detergent products is extremely sensitive to surfactant crystalline morphology. As environmental pressure leads to changes in permissible surfactant choice, a detailed understanding of surfactant crystallisation will aid reformulation and redesign of the process. Straight-chain saturated sodium soaps were chosen as model systems for our studies as

they represent typical examples of natural surfactants.

Our research program seeks to characterise and interrelate the crystal structure, external morphology and growth kinetics of triglycerides and surfactant systems. We have developed a new *in-situ* cell for X-ray studies which permits the examination of long-chain hydrocarbon samples under conditions of well controlled stirring/agitation and has the capability for very rapid cooling/heating (*ca.* 10°C/min). This rheometer cell design incorporates an optical light probe to detect nucleation. We have used this and other X-ray cells for time-resolved combined small and wide angle X-ray scattering studies on station 16.1 in order to investigate *in-situ* the crystallisation process of fats and surfactants. A polymorphic phase transition was observed for cocoa butter under conditions of shear during a cooling/heating cycle. For anhydrous sodium myristate at least 8 phase transitions were observed. Sodium laurate was crystallised from a hexagonal liquid crystalline phase in order to study the descent through the liquid crystalline phases to the resulting coagel phase. The poster will outline our *in-situ* crystallisation data together with a description of the X-ray cells used.

## Two-Dimensional Detector Calibration and Data analysis with FIT2D

A P Hammersley<sup>1</sup>, T Wess<sup>2</sup>, and L Wess<sup>2</sup>.

<sup>1</sup>ESRF, BP220, Grenoble 38043, France.

<sup>2</sup>University of Stirling, Stirling, U.K.

Detector calibration and data correction is of utmost importance for extracting high quality quantitative results from modern area detectors. Non-linearity of intensity response, spatial distortion, and non-uniformity of intensity response, and for imaging plates decay of latent signal during scanning, can all be corrected using the program FIT2D [1,2].

Major progress has been made in the correction of non-uniformity of intensity response (flat-field correction). A fluorescence sample at the crystallographic sample position provides a "flood-field" illumination of the detector from a very small source volume (similar to the sample). The source intensity distribution, which is not quite isotropic, is characterised with a two-theta scan. FIT2D allows "flood-field" detector images to be corrected to "flat-field" images, which are used for flat-field correction of scientific data [3].

New data analysis developments have been made in the field of Powder Diffraction (with 2-D detectors). These developments can also be interesting for fibre diffraction e.g. arbitrary pixel size re-binning (transformation) to polar coordinates.

1. A P Hammersley, S O Svensson, and A Thompson, Nucl. Instr. Meth., **A346**, 312-321, (1994)
2. A P Hammersley, S O Svensson, and A Thompson, H Graafsma, Å Kvick, and J P Moy, Rev. Sci. Illstr., (SRI-94), March, (1995)
3. J-P Moy et al, in preparation

### Solving Frame 1 of "Muscle - the Movie": Myosin Head Arrangement in Relaxed Bony Fish Muscle.

J.J. Harford, L. Hudson, R. Denny and J.M. Squire

Biophysics Section, Blackett Laboratory, Imperial College, London SW7 2BZ, UK.

Low-angle 2-D X-ray diffraction patterns from bony fish muscle (Harford *et al* (1994) *J.Mol.Biol.* **239**, 500-512) contain sufficient information to allow modelling using the known myosin head shape. A series of 2-D diffraction patterns has been recorded at 5 ms time intervals during a typical tetanic contraction of plaice fin muscle (Harford & Squire (1992) *Biophys.J.* **63**, 387-396). The problem of separating the well-defined Bragg peaks from the asymmetric, smooth background to give reliable intensities ( $I(hkl)$ ) for the Bragg peaks has been tackled using new CCP13 software. A new program has also been written to read in the stripped  $I(hkl)$  values and the head shape and to search over parameter space (head orientation, tilt, rotation, radius etc) to give the best R-factor or correlation coefficient values between observed and calculated intensities. Refinement procedures are being used to optimise the modelling. Results to date indicate that, although quite good agreement with the observed data can be obtained from the myosin heads alone. When the basic modelling is established, structure refinement will proceed by combining model phases and observed amplitudes in a Fourier difference synthesis. The final relaxed fish muscle structure can then be used as part of a boot-strapping exercise to define the fish muscle unit cell contents as force is gradually generated through the tetanic contraction. This will provide a time sequence of images from which to compile 'Muscle - The Movie'. Included in this will be modelling of the actin filament structure during activation, including both the tropomyosin shift and actin sub-domain movements (Squire *et al* (1994) *Biophys. Chem.* **50**, 87-96). [Work Supported by BBSRC & MRC].

### Fast Time-Resolved X-ray Diffraction Studies of Fish Muscle using the Fast 1-D Multiwire Detector

J.J.Harford, L. Hudson, R. Denny and J.M.Squire

Biophysics Section, Blackett Laboratory, Imperial College, London SW7 2BZ, UK.

In order to improve the time and spatial resolution of our X-ray diffraction studies of the bony fish equatorial pattern (Harford & Squire (1992) *Biophys.J.* **63**, 387-396; Harford *et al* (1994) *J.Mol.Biol.* **239**, 500-512), as part of our study of the molecular events involved in force production (Squire *et al* (1994) *Biophys. Chem.* **50**, 87-96), measurements were carried out on beam line 16.1 at the SRS using the new fast 1-D multiwire detector. We have previously produced a 10ms time-resolved sequence of the density changes viewed down the muscle fibre axis by Fourier synthesis using the first five orders of equatorial diffraction, corresponding to about 13nm spatial resolution. It has been possible using the CCP13 software developed at Daresbury to extract meaningful intensities to about 6nm so far from multiwire area detector images. Counting statistics for the 10 equatorial reflections from one muscle summed over 30 tetani recorded at 1ms time-resolution were just greater than 1%. There is a small decrease in the spacing of the 10 reflection (0.3%) accompanying contraction and this parameter and the increase in the peak width show a 5 to 10ms lead with respect to the intensity. It should be possible to improve the time-resolution of our 2-D molecular movie by at least a factor of two and with phases from our present modelling of the 3-D structure to improve the spatial resolution by a similar factor. [Work Supported by BBSRC & MRC].

### Neutron Fibre Diffraction Studies at the ILL

Paul Langan

Institut Laue Langevin, BP 156, 38042 Grenoble Cedex France.

At the beginning of this year, after a temporary shutdown of almost four years, the ILL restarted as the world's most intense dedicated neutron source. A brief review of the wide range of neutron diffraction

techniques being used to study fibre structures and dynamics will be given, with particular emphasis on high angle diffraction.

The potential of this technique is dependent on developments in a number of areas, two of which will be discussed;

1. The efficient coverage of large continuous volumes of reciprocal space simultaneously. For this reason fibre studies now account for around 25% of beam time on the high flux single crystal diffractometer which is equipped with a large position sensitive detector, D19.

2. The exploitation of the difference in scattering length of hydrogen and deuterium. In particular novel deuteration techniques for biological molecules are opening up exciting possibilities.

### An X-ray Diffraction Study of the 14.34nm Meridional Reflection during the Contractile Cycle of Live Frog Muscle

C.V.Miles<sup>1</sup>, J.Gandy<sup>2</sup>, J.Bordas<sup>2</sup>, R.Denny<sup>3+4</sup>, G.P.Diakun<sup>4</sup>, J.Lowys, G.R.Mant<sup>4</sup>, A.Svensson<sup>1</sup>, E.Towns-Andrews<sup>4</sup>

<sup>1</sup>Department of Physics, Leicester University;

<sup>2</sup>Department of Physics, Liverpool University;

<sup>3</sup>Imperial College, London;

<sup>4</sup>EPSRC-DRAL Daresbury Laboratory;

<sup>5</sup>Open University, Boars Hill, Oxford

We have been investigating the two-dimensional high resolution low angle X-ray diffraction patterns from whole frog sartorius muscles in isometric and isotonic contractions and at rigor. One-dimensional time resolved meridional data were also collected.

As has recently been shown (Bordas et al, Biophys.J, in press) at the peak of isometric contraction the third order myosin meridional reflection is resolved into two closely overlapping peaks at 1/14.42nm and 1/14.62nm, indicating that the myosin heads occupy two distinct head configurations. During isometric contraction and quick releases two peaks are visible, one of which follows the same time course as tension generation. But when the release is extended to suppress tension generation, the reflection returns to a single peak at the rest periodicity.

After studying the spacing and intensity time courses of the individual peaks during these experiments, we believe that this split is not caused by interference effects, but is a genuine feature arising from two

individual myosin head populations with slightly different but distinct axial configurations.

### Structure & Crystallisation Kinetics of Diblock Copolymers Containing a Crystallisable Block.

A. J. Ryan<sup>1</sup>, S. Naylor<sup>1</sup>, P. Fairclough<sup>1</sup>, I.W. Hamley<sup>2</sup>, C. Booth<sup>3</sup>, F.S. Bates<sup>3</sup>, R. Register<sup>4</sup>, P. Ranjaran<sup>5</sup> and W. Bras<sup>6</sup>

<sup>1</sup>Manchester Materials Science Centre, UMIST

<sup>2</sup>Durham University

<sup>3</sup>Manchester University

<sup>4</sup>University of Minnesota, USA

<sup>5</sup>Princeton University, USA

<sup>6</sup>AMOLF, The Hague, The Netherlands

As part of our research programme into the phase behaviour of diblock copolymers [1] we have initiated a programme of study into semicrystalline block copolymers. Time-resolved simultaneous synchrotron small-angle and wide-angle X-ray scattering (SAXS and WAXS) and DSC experiments have been performed on poly(ethylene)-poly(ethyleneethylene) [2,3], poly(ethylene)-poly(ethylene-propylene) [2,3] and poly(ethylene)-poly(hthpropylene) [4] diblock copolymers quenched from melts with lamellar and hexagonal-packed cylinder structures. A series of polyether based copolymers close to the order disorder transition have also been synthesised by anionic polymerisation and studied by SAXS/WAXS/DSC [5]

We find that the original microphase separated morphologies are destroyed due to poly(ethylene) (PE) chain folding upon crystallization. Below the melting temperature, samples with a volume fraction  $f_{PE} \approx 0.5$  form lamellar structures distinct from that in the melt. On quenching hexagonal  $f_{PE} = 0.25$  samples form a lamellar structure similar to that of the  $f_{PE} = 0.49$  sample, whilst the hexagonal-packed cylinder structure of an  $f_{PE} = 0.75$  sample is also destroyed by crystallization but does not form well ordered lamellae.

The evolution of structure from the disordered melt to the ordered melt and then to the semicrystalline solid has been studied. The SAXS profiles from crystallized materials are shown to correspond to the sum of scattering from block copolymer lamellae, with up to four orders of reflection, plus a broad peak arising from semicrystalline PE. Analysis of scattering density correlation functions calculated using the SAXS data shows that the PE lamellae thickness is

(45±10) Å for all samples, similar to that observed for PE homopolymer. The WAXS data reveal that PE crystallizes in its usual orthorhombic form in all samples. The relative degree of crystallinity as a function of time after a quench, determined from the SAXS invariant, is fitted by Avrami equations for spherulitic crystallite growth. The Avrami exponent is found to be  $n=(3.0\pm 0.1)$  for all samples (14 polymers), consistent with crystallisation to form a spherulitic morphology by a nucleation and growth process.

## References

1. S. Forster, A.K. Khandpur, J. Zhao, F.S. Bates, I.W. Hamley, W. Bras and A.J. Ryan *Macromolecules*, **27**, 6922 (1994).
- 2 A.J. Ryan, I.W. Hamley, W. Bras and F.S. Bates *Macromolecules*, **28**, *in press* ( 1995).
- 3 P. Ranjaran, R.A. Register, D.H. Adamson, L.J. Fetter, W. Bras, S. Naylor and A.J. Ryan *Macromolecules*, **28**, 1422 (1995).
- 4 P. Ranjaran, R.A. Register, D.H. Adamson, L.J. Fetter, W. Bras, S. Naylor and A.J. Ryan *Macromolecules*, **28**, *in press* (1995).
5. Y-W Yang, S. Tanodekaew, S-M Mai, C. Booth, A. J. Ryan, W. Bras, K. Viras *Macromolecules*, **28**, accepted Feb (1995)

## Morphology of bulk and oriented gels of triblock copolymers as observed by small-angle scattering.

K Reynders, N Mischenko, M.H.J. Koch<sup>1</sup>,  
K Moltensen<sup>2</sup>, H Reynaers

Laboratorium voor Macromoleculaire Structuurchemie,  
Departement Scheikunde, Katholieke Universiteit Leuven,  
Celestijnenlaan 200 F, B3001 Heverlee, Belgium

<sup>1</sup> EMBL-Outstation c/o DESY, Notkestrasse 85, D-22603  
Hamburg, Germany

<sup>2</sup> Department of Solid State Physics, Risø National  
Laboratory, DK4000 Roskilde, Denmark

Gels of triblock copolymers display superstructures consisting of domains of associated endblocks, connected by the midblocks dissolved in an extender oil (physical network). The endblock used is polystyrene (PS), while the rubber midblock is either polyethylene/propylene (PS-P/EP-PS) or polyethylene/butylene (PS-P/EB-PS). The ordering of the PS domains is a function of block copolymer concentration, molar mass, end/midblock ratio, deformation and/or external pressure and temperature. The scattering patterns of the isotropic samples are fitted with two different models: a hard sphere liquid model and

a model of a disordered solid with local coordination. At moderate (25-100%) stretching two different scattering effects are derived from experimental observations. The first one is the change from a circular interdomain interference ring to an elliptical band which represents the stretching of the first coordination spheres of the PS domains, regarded here as "basic units". The second effect is the appearance of diffraction spots which are assigned to an increase of correlation between the basic units (formation of a layered structure). At higher (150-1000%) deformations the SAXS pattern is gradually transformed into a "butterfly" type scattering pattern with a pronounced scattering-free stripe perpendicular to the stretching direction. Preparation of gel films by high-pressure (40 MPa) molding at elevated temperatures can cause a preorientation effect which further develops by high-pressure (0.1-0.7 GPa) treatment. These observations point to the cluster character of the physical network in the gel.

## The Effect of Fibres on the Solidification Processes That Occur During The Reactive Processing of Polymer Composites

Steven Naylor, Anthony J. Ryan, Phillip T. Draper, John L. Stanford, Michael J. Elwell, Arthur N. Wilkinson<sup>2</sup>, Wim Bras<sup>3</sup> and Bernd U. Komanschek<sup>4</sup>

<sup>1</sup>Manchester Materials Science Centre, UMIST, Grosvenor Street, Manchester, M1 7HS, UK.

<sup>2</sup>Department of Materials Technology, Manchester Metropolitan University, Oxford Road, Manchester, M1 5GD, UK.

<sup>3</sup>AMOLF, Kruislaan 407, 1098 SJ Amsterdam, The Netherlands, UK.

<sup>4</sup>Daresbury Laboratory, Keckwick Lane, Warrington, WA4 4AD, UK.

Simultaneous SAXS/WAXS has been used to study the structure development in polyurethanes. Reactive materials based on polyurethane elastomers and rigid isocyanurate materials have been investigated as a function of mould temperature with and without fibres in the X-ray path.

The poly(urethane-urea)-forming system has a two stage reaction, which is characterised by macrophase separation followed by microphase separation. The presence of glass fibres appeared to accelerate the rate of structure development in this system at temperatures of between 105 and 120°C. The most probable mechanism responsible for this increase in growth-rate is surface-induced crystallisation around the fibres, which will be further studied by a combination of 2D SAXS/WAXS, optical microscopy and

birefringence measurements.

Cyclo-trimerisations used in the formation of poly-isocyanurates are very fast and, as such, the material experiences a deep quench. It is shown that, as a result of this, spinodal decomposition, rather than nucleation and growth, is the mechanism responsible for microphase separation during the formation of the poly(isocyanurate-urea) system

## X-ray Diffraction Studies of Lyotropic Liquid Crystals

Gordon J.T. Tiddy

Dept. of Chemistry and Applied Chemistry, University of Salford

Arguably the most important class of lyotropic liquid crystals is that comprised of ordered solute aggregates formed by self-association, usually in water. There are two major types, amphiphilic mesophases formed by surfactants and chromonic mesophases formed by flat, polar, polarisable, polyaromatic materials (which frequently are used as dyes or drugs). Both types are commercially important as well as offering the opportunity to study fundamental questions concerning molecular interactions and the nature of phase transitions.

For surfactant systems, major outstanding questions are:

- (i) The structure of mesophases with aggregate curvature intermediate between hexagonal and lamellar phases.
- (ii) The structure and swelling behaviour in very dilute systems, including those of semi-solid "gel" phases.
- (iii) Partial miscibility within mesophases.

With the chromonic systems many basic problems remain to be solved. These include:

- (i) Long range mesophase structure
- (ii) Molecular packing within aggregates
- (iii) The nature of phase transitions.

Examples of these problems investigated using the Synchrotron diffraction facilities will be discussed.

## Refinement of the fd filamentous bacteriophage coat protein using maximum entropy

L. C. Welsh<sup>1</sup>, M. F. Symmons<sup>2</sup>, C. Nave<sup>3</sup>, E. Marseglia<sup>1</sup>, D. A. Marvin<sup>2</sup> & R. N. Perham<sup>2</sup>

<sup>1</sup> Cavendish Laboratory.

<sup>2</sup> Department of Biochemistry, University of Cambridge.

<sup>3</sup> Daresbury Laboratory.

The virion of fd filamentous bacteriophages is a flexible nucleoprotein rod 6nm in diameter and 880nm long, with a shell of  $\alpha$ -helical protein subunits surrounding a core of DNA. X-ray diffraction from magnetically aligned fibres of the native and iodinated Y21M mutant of the fd strain of bacteriophage gives patterns with layer-lines that can be measured to a resolution of about 3.3Å. Quantitative intensity data have been extracted from such patterns and used to calculate electron density maps of the fd major coat protein using a maximum entropy method. The helical symmetry of fd is such that on a given layer-line at a given resolution there are a number of overlapping Bessel function terms. The maximum entropy method that we are using can separate and phase the Bessel function terms using only native intensity data and a low resolution prior electron density map. We have tested the performance of the maximum entropy method in this task using simulated data from the current model of the fd major coat protein. We have also tested by simulation various methods for using maximum entropy in the refinement of the fd major coat protein model against fibre diffraction data. In the light of the results of these simulations we are now refining the fd model against the observed fibre diffraction data.

## X-ray fibre diffraction and molecular models of Pf3 filamentous bacteriophage.

L. C. Welsh<sup>1</sup>, M. F. Symmons<sup>2</sup>, C. Nave<sup>3</sup>, E. Marseglia<sup>1</sup>, D. A. Marvin<sup>2</sup> & R. N. Perham<sup>2</sup>

<sup>1</sup> Cavendish Laboratory

<sup>2</sup> Department of Biochemistry, University of Cambridge;

<sup>3</sup> Daresbury Laboratory.

The major coat protein of the Pf3 strain of filamentous bacteriophage has been extensively studied in membrane environments but knowledge of the virion structure is underdeveloped relative to that of other strains of filamentous phage. However, the current data indicate that the Pf3 virion has a number of unusual properties. We have collected wide-angle diffraction patterns from magnetically aligned fibres

of Pf3 and these have confirmed earlier suggestions that this strain has a class II helix symmetry. In fact the observed patterns are very similar to those of the high temperature form of the well-studied Pfl strain. Despite the similarities to Pfl as regards the coat protein symmetry and structure, the packing of the DNA in the two strains must be very different as Pf3 has a nucleotide/coat protein subunit ratio about 2.4 times that of Pfl. Furthermore Pf3 does not show a temperature dependent phase transition analogous to that in Pfl, as determined from both DSC and fibre diffraction. We have built initial molecular models of the Pf3 major coat protein, based on the high-temperature model of Pfl, and checked their validity by various methods including the simulation of fibre diffraction patterns. We will refine these models against the observed fibre diffraction data using techniques developed for the refinement of the fd strain of filamentous bacteriophage.

### The Structure of an Avian Cartilage. A Combined X-ray and Biochemical Analysis

Tim Wess \*, Linda Wess\*, Andy Hammersley° and Paul Hocking<sup>†</sup>

\* Department of Biological and Molecular Sciences, University of Stirling, Stirling FK9 4LA, Scotland, U.K.

° ESRF, BP 220, F-38043, Grenoble CEDEX, FRANCE

<sup>†</sup> Division of Environment and Welfare, Roslin Institute (Edinburgh), Roslin, Midlothian, EH25 9PS, Scotland, U.K

Cartilage is susceptible to degenerative changes, this is of commercial and welfare importance in the poultry industry. X-ray diffraction has been used to determine the orientation of collagen fibrils at a variety of depths in cartilage. A complimentary biochemical assessment of collagen type with respect to penetration from the articulating surface towards the bone at 20 micron intervals has been made. X-ray diffraction of antitrochanter (hip) joints was conducted using synchrotron radiation at DRAL and ESRF synchrotrons with a beam size of 200 microns to examine the antitrochanter of turkeys aged from 8-60 weeks at 10 week intervals. The arced distribution of intensity from equatorial reflections was used to determine the parameter  $g(\phi)$ , a probability distribution for the fibril orientation. Biochemically two main regions of the antitrochanter were found. The surface region of the articulating surface to a depth of 1.2 mm was type I collagen as judged by the CNBr digest pattern on PAGE gel electrophoresis. This corresponded with X-ray diffraction patterns indicating relatively well aligned fibrils of collagen (half height of  $g(\phi)$ ) +/- 30 degrees). The surface portion showed a higher

degree of disorientation indicating that a different architecture of fibril organisation may occur at the surface. The change from type I to type II collagen was abrupt (less than 20 micron) and the underlying cartilage exhibited a much reduced orientation profile indicating that fibril orientation was close to isotropy. Further changes in fibril organisation were observed close to the interface with the ossified

### Novel Experiments in Polymer Science by Means of Synchrotron Radiation: On-Line Fiber spinning, Microfocus X-ray Diffraction and Grazing Incidence Diffraction.

H.G. Zachmann

Institut für Technische und Makromolekulare Chemie,  
University of Hamburg, Bundesstr. 45, D-20146 Hamburg,  
Germany

Three types of experiment in the application of synchrotron radiation to polymer science have been performed by us recently. (i) An extruder and a take-up device suitable for spinning of fibers at speeds up to 4000 m/min has been set up at HASYLAB in Hamburg. The development of wide-angle X-ray scattering (WAXS) and small angle X-ray scattering (SAXS) along the fibre was measured and related to the temperature and diameter profile. It was shown that SAXS appears before crystal reflections become visible. It was also shown that crystallization starts at the beginning of the neck-like deformation. (ii) By using a microfocus camera at the ESRF in Grenoble, the local change of molecular orientation in a nematic liquid crystalline polymer was determined. It was shown that it is possible to investigate the nature and arrangement of the disclinations by using this method. Furthermore one can determine local changes in chain orientation in oriented conventional polymers as well as local changes of structure within spherulites. (iii) A goniometer for measuring the grazing incidence diffraction in vacuum was constructed at HASYLAB. This scattering from 400 Å thick films obtained by spin coating of different polymers was measured before and after crystallization. Among other things, the influence of the spin coating speed on the orientation of the crystals was determined.

## The 5th Annual CCP13/NCD Workshop

**“Diffraction from Fibres and Polymers”**

Tuesday 7th to Thursday 9th May 1996  
Daresbury Laboratory

Keynote speakers:

George Wignall and David Hukins

For further details please contact The Conference Office, Daresbury Laboratory, Warrington, Cheshire, WA4 4AD. (Tel: 01925 603235. Fax: 01925 603195 Email: conference@dl.ac.uk)

## The 17th IUCR General Assembly and International Congress of Crystallography

**“Fibre Diffraction SIG Meeting”**

8th to 17th August 1996  
Seattle, Washington, USA

For further details please contact Professor R.F.Bryan, Department of Chemistry, University of Virginia, Charlottesville, VA 22903, USA.

## X International Conference on Small-Angle Scattering

21st to 25th July 1996  
Campinas, Brazil

For further details please contact Professor Aldo Craievich, LNLS, Cx. Postal 6192, 13081-970 Campinas, SP, Brazil.

# Synchrotron X-Rays *in* Medicine



CENTRAL LABORATORY OF THE  
RESEARCH COUNCILS

***What are they and are they of any use?***

***Find out at a meeting to inform and encourage research  
to be held at***

***Daresbury Laboratory, England, 2-3 May 1996***

## Background

Daresbury Laboratory houses the Synchrotron Radiation Source, the UK's only source of Synchrotron x-rays. Various techniques which utilise Synchrotron x-rays can yield very detailed diagnostic information from a wide variety of tissue types. The object of the conference is to explore the exciting research and clinical possibilities offered by synchrotron radiation and to inform clinicians about the various techniques in common use.

The meeting consists of an informative session to explain what Synchrotron Radiation is, followed by 5 medical sessions which are designed to stimulate ideas and examine new diagnostic techniques. There will be reports of projects already underway, both in the UK and abroad, and discussions of existing medical problems where Synchrotron x-rays may contribute.

## Programme

*There will be sessions on the following subjects, the session Chairmen are shown in brackets*

Synchrotron Radiation	(Prof. P. Lindley, Daresbury)
Neurology	(Prof. A. Jackson, Manchester)
Soft Tissue	(Prof. A. Miller, Stirling)
Bone	(Prof. J. Adams, Manchester)
Mammography	(Dr. C. Boggis, Manchester)
Cardiology and Vascular	(Dr. R. Coulton, Papworth)

In addition there will be summing up by Prof. I. Isherwood and a tour of Daresbury Laboratory including the Synchrotron Radiation Source.

Further information from;  
The Conference Office  
The Daresbury Laboratory  
Warrington, WA4 4AD, England  
Telephone 44 (0)1925 603235  
Fax 44 (0)1925 603195  
Email conference@dl.ac.uk  
WWW: <http://ncdfs1.dl.ac.uk/SRXIM/srxim.html>

\*\*\*\*\*

## **CCP13 TRAVELLING FELLOWSHIPS**

CCP13 Travelling Fellowships (£500) are intended to supplement awards to younger UK researchers travelling abroad for a conference involving fibre diffraction in order to give them the opportunity to visit a few fibre diffraction laboratories in the host Country. The £500 is intended to cover the extra travel, accommodation and subsistence costs in the host Country involved in visiting these laboratories. The recipients will be asked to report on their visits in a talk to the May Annual Meeting of CCP13 and also to contribute a short (1 page) report for the annual 'CCP13 Newsletter'. Current PhD students must have their application countersigned by their research supervisor if they wish it to be considered. TWO awards will be made each year.

***Application deadline for travel in Summer 1996: MARCH 31st 1996***

Application forms can be obtained from the CCP13 secretary, Dr. G. Mant (g.r.mant@dl.ac.uk).

If awarded, the scholarship will be sent by cheque, once the travel arrangements of the Fellow have been confirmed.

\*\*\*\*\*

## **CCP13 VISITING SCIENTIST PROGRAM**

From time to time the CCP13 Committee will invite an outstanding scientist from overseas to take part in the May Annual CCP13/NCD Workshop and, before or after the Workshop, to visit various contributing laboratories in the UK over a period of one or two weeks to talk to and advise on fibre diffraction methods and results.

CCP13 members are welcome to put forward to the Committee the names and addresses of possible visitors, preferably with some details in writing, including suggestions about which UK scientists/laboratories should be visited.

\*\*\*\*\*

# SIEMENS

## Finally – an easy-to-use X-ray diffraction system for analyzing polymers

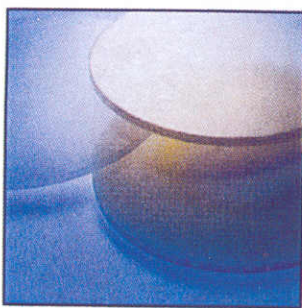
The Siemens Area Detector and GADDS (General Area Detector Diffraction System) polymer software are faster, more flexible and easier to run than any other X-ray diffraction system available today. Featuring pop-up menus and real-time color display as part of a graphics-oriented user interface, the only thing missing is competition.

- Ideal for texture analysis, percent crystallinity and other applications, including QC
- Easily measures d-spacings, angles and intensities from any pixel location
- Versatile data files can be used with powder diffraction software for phase identification and profile fitting



### Plastics

True QC instrument for measuring intensities and d-spacings resulting from different draw rates or annealing temperatures



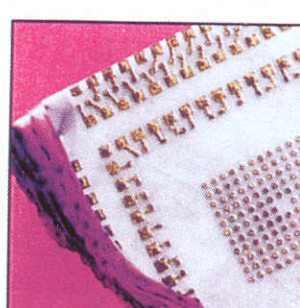
### Texture

Measures scattering from amorphous through polycrystalline to 3-D single-crystalline with a powerful scripting feature



### Composites

Versatile analysis of composite bondings with use of the system as an X-ray probe





Produced by  
CCLRC  
Daresbury Laboratory  
for CCP13

